Correlation of blood flow in a packed bed of glass spheres
by Richard Dale Mountain

A thesis submitted to the Graduate Faculty in partial fulfillment of the requirements for the degree of
MASTER OF SCIENCE in Chemical Engineering
Montana State University

Abstract:
The flow of blood in the human body is complicated by the complex non-Newtonian rheology of blood and the complex nature of the circulatory system. Recent attempts to quantitatively understand in vivo blood flow have raised many questions concerning the dynamics of blood flow both on a macroscopic level and a microscopic level. In an attempt to systematically approach some of the problems that need to be resolved the steady, laminar flow of human blood in a packed bed of glass spheres has been studied.

A capillary model to correlate the macroscopic flow of blood in a packed column was developed assuming that each pore could be viewed as a single straight tube. The Rabin-owitsch-Mooney relation describing non-Newton.ian flow in a straight pipe was modified and used to estimate an appropriate shear rate within the bed. The shear stress within the bed was estimated similarly and then shear stress and shear rate used to define a mean effective viscosity. This viscosity was then used to modify existing correlations describing Newtonian flow in a packed bed.

Blood flow was examined at modified Reynolds numbers ranging from 2.2x10-3 to 3.6x10-1 indicating laminar flow. Application of the capillary model yielded results that fit-a modified Kozeny-Carman equation with an average error of 1.87%.

Shear rate-viscosity data obtained from application of the capillary model were compared to actual viscometer data. It was found that experimental calculations yielded viscosities considerably lower than viscometer data at comparable shear rates. This discrepancy was minimized at shear rates sufficiently high to produce Newtonian behavior.

I It was concluded that the capillary model is an effective and powerful tool for correlating the macroscopic flow of blood in a packed bed since the method is independent of hematocrit and viscometer data. However, the method apparently fails to accurately predict and explain the microscopic flow of blood through the pores of the bed due to a breakdown of continuum mechanics.

Statement of Permission to Copy

In presenting this thesis in partial fulfillment of the requirements for an advanced degree at Montana State University, I agree that the Library shall make it freely available for inspection. I further agree that permission for extensive copying of this thesis for scholarly purposes may be granted by my major professor, or, in his absence, by the Director of Libraries. It is understood that any copying or publication of this thesis for financial gain shall not be allowed without my written permission.

Signature Richard D. Mountain

Date July 26, 1973

CORRELATION OF BLOOD FLOW IN A PACKED BED OF GLASS SPHERES

by

RICHARD DALE MOUNTAIN

A thesis submitted to the Graduate Faculty in partial fulfillment of the requirements for the degree

of

MASTER OF SCIENCE

in

Chemical Engineering

Approved:

L Lloyd Berg
Head, Major Department

John R. Lockett
Chairman, Examining Committee

Henry L Parsons
Graduate Dean

MONTANA STATE UNIVERSITY
Bozeman, Montana

August 1973

ACKNOWLEDGMENT

The author wishes to thank the faculty of the Montana State University Department of Chemical Engineering for their advice and assistance. A special note of thanks must go to Dr. Giles R. Cokelet who invariably provided both the theoretical proficiency and practical ingenuity necessary for completion of this research.

The author received a National Science Foundation Traineeship for the period September 1972 to September 1973. This, and other assistance provided by Montana State University, has been greatly appreciated.

TABLE OF CONTENTS

INTRODUCTION 1

THEORETICAL CONSIDERATIONS 10

Newtonian Flow Through Packed Beds 10

Non-Newtonian Flow and the Capillary Model 12

EXPERIMENTAL APPARATUS AND PROCEDURE 22

Experimental Apparatus 22

Blood 25

Bead Analysis 25

Syringe Pump Calibration 26

Transducer Calibration 28

Entrance and Wall Effects 31

Determination of Void Fraction 33

EXPERIMENTAL RESULTS AND DISCUSSION 35

Correlation of Newtonian Flow 35

Effective Pore Diameter 37

Correlation of Blood Flow 40

The Packed Bed as a Viscometer 53

Recommendations for Further Work 61

CONCLUSIONS 63

TABLE OF CONTENTS (continued)

APPENDIX 64

Derivation of Rabinowitsch-Mooney Relation 65

LITERATURE CITED 70

LIST OF TABLES

I	Correlation of Newtonian water flow	36
II	Determination of effective pore diameter from Newtonian flow of water	39
III	Application of capillary model to blood flow, hematocrit=16.8%	41
IV	Application of capillary model to blood flow, hematocrit=34.5%	42
V	Application of capillary model to blood flow, hematocrit=48.5%	43
VI	Application of capillary model to blood flow, hematocrit=40.3% plus 0.5% Dextran	44
VII	Correlation of blood flow, hematocrit=16.8%	45
VIII	Correlation of blood flow, hematocrit=34.5%	46
IX	Correlation of blood flow, hematocrit=48.5%	47
X	Correlation of blood flow, hematocrit=40.3% plus 0.5% Dextran	48

LIST OF FIGURES

1	General behavior of Newtonian flow through packed beds	13
2	General schematic diagram of experimental apparatus	23
3	Schematic diagram of column used	24
4	Photomicrographs of glass beads	27
5	Schematic diagram of transducer calibration apparatus	29
6	Transducer calibration data	30
7	Experimental set-up utilized to examine possible entrance effects	32
8	Modified friction factor vs. modified Reynolds number for laminar Newtonian flow of water	38
9	Modified friction factor vs. modified Reynolds number for laminar blood flow through a packed bed	51
10	Blood viscosity vs. shear rate as calculated by capillary model	54
11	Comparison of experimental calculations to viscometer data, H=16.8%	56
12	Comparison of experimental calculations to viscometer data, H=34.5%	57
13	Comparison of experimental calculations to viscometer data, H=48.5%	58

ABSTRACT

The flow of blood in the human body is complicated by the complex non-Newtonian rheology of blood and the complex nature of the circulatory system. Recent attempts to quantitatively understand *in vivo* blood flow have raised many questions concerning the dynamics of blood flow both on a macroscopic level and a microscopic level. In an attempt to systematically approach some of the problems that need to be resolved the steady, laminar flow of human blood in a packed bed of glass spheres has been studied.

A capillary model to correlate the macroscopic flow of blood in a packed column was developed assuming that each pore could be viewed as a single straight tube. The Rabinowitsch-Mooney relation describing non-Newtonian flow in a straight pipe was modified and used to estimate an appropriate shear rate within the bed. The shear stress within the bed was estimated similarly and then shear stress and shear rate used to define a mean effective viscosity. This viscosity was then used to modify existing correlations describing Newtonian flow in a packed bed.

Blood flow was examined at modified Reynolds numbers ranging from 2.2×10^{-3} to 3.6×10^{-1} indicating laminar flow. Application of the capillary model yielded results that fit a modified Kozeny-Carman equation with an average error of 1.87%.

Shear rate-viscosity data obtained from application of the capillary model were compared to actual viscometer data. It was found that experimental calculations yielded viscosities considerably lower than viscometer data at comparable shear rates. This discrepancy was minimized at shear rates sufficiently high to produce Newtonian behavior.

It was concluded that the capillary model is an effective and powerful tool for correlating the macroscopic flow of blood in a packed bed since the method is independent of hematocrit and viscometer data. However, the method apparently fails to accurately predict and explain the microscopic flow of blood through the pores of the bed due to a breakdown of continuum mechanics.

INTRODUCTION

Recent advances in medicine and physiology, particularly the increased impetus to understand cardiovascular anomalies on a more scientific basis, have made it desirable to quantitatively understand the dynamics of blood as it flows through the human circulatory system. Indeed, maintenance of all aspects of homeostasis in the human body depends, to some extent, on the circulation. Thus, as medicine continues its radical transistion from art to science, it becomes increasingly important to be able to accurately predict how changes in microscopic and macroscopic properties will affect blood flow. However, an accurate correlation of blood flow in the human body is, in general, complicated by two factors: 1) The complex non-Newtonian rheology of human blood; and, 2) the variable and complex geometry of the circulatory system.

The complex rheology of human blood is due to its unique chemical and physical properties that enable it to fulfill its essential role as the medium of transport within the body. Essentially, blood consists of specialized cellular structures; erythrocytes, leukocytes, and thrombocytes, suspended in an extracellular liquid medium; the blood plasma.

The erythrocyte (red blood cell) is a biconcave disc with a mean diameter of 8.5 microns and a maximum thickness of approximately 2.4 microns. The red cell membrane consists of proteins, lipids, and mucopolysaccharides that collectively confer certain antigenic properties and blood group specificity. Hemoglobin, the conjugated protein that functions in oxygen transport, is found within the red cell along with various electrolytes, enzymes, and metabolites. Erythrocytes constitute by far the majority of the formed elements and cause the non-Newtonian rheology of blood.

Leukocytes (white blood cells) and thrombocytes (platelets) function as a defense against infections and as a factor in blood clotting respectively. They constitute only a minute fraction of the formed elements and are thus considered not to significantly affect blood rheology.

Blood plasma is a complex solution containing approximately 90% water by weight. Its major solute is a group of heterogeneous proteins including albumin, antibodies, hormones, and clotting agents. Blood plasma also contains carbohydrates, lipids, and various electrolytes. Plasma, per se, is a Newtonian fluid.

The preceding description of blood has been intentionally brief and generalized; an attempt only to provide the

broad anatomical basis for viewing blood as a suspension of deformable particles (i.e., erythrocytes) that results in complex non-Newtonian rheology.

An accurate and complete quantitative description of blood rheology has evolved only within the past decade. It is due largely to the development of more accurate and complex laboratory instrumentation in the hands of experimenters sufficiently versed in fluid dynamics in general and rheology in particular to comprehend the limitations of the instruments and to accurately convert raw data into meaningful rheological parameters. Thus, it is useful to briefly outline currently accepted concepts of human blood rheology before defining and exploring the experimental problem presented in this paper. More detailed reviews of blood rheology have been given by Cokelet(1972), Merrill(1969), Wayland (1967), and Whitmore(1968).

Several investigators (Cokelet, 1963; Charm and Kurland, 1965; Merrill and Pelletier, 1967; Brooks, et al, 1970) have provided extensive experimental evidence showing that under certain conditions human blood exhibits non-Newtonian behavior; that is, the relationship between shear stress and shear rate is non-linear so the viscosity is, in general, dependent upon shear rate. Specifically, blood is non-

Newtonian at lower shear rates with a gradual transistion to Newtonian behavior at higher rates of shear. The point of transition depends to a large extent on hematocrit (defined as the per cent, by volume, of formed elements); the greater the hematocrit, the larger the rate of shear necessary to produce Newtonian behavior. This phenomenon can be qualitatively explained as follows: At low shear rates the red blood cells aggregate producing a fluid of greater viscosity; as the rate of shear increases the aggregation of cells decreases resulting in a decrease in viscosity. Eventually the shear rate is sufficient to prevent any aggregation of cells and Newtonian behavior is observed.

As well as shear rate and hematocrit, blood viscosity depends upon temperature and also more subtle factors such as concentration of plasma proteins and the physiological state of the erythrocyte. This latter factor is extremely difficult to control since even in the presence of a suitable anticoagulant erythrocytes removed from the body undergo gradual loss of adenosine triphosphate (ATP) with a subsequent change to a hardened, crenated form with radically different rheological behavior.

It should be noted that several investigators (Cokelet, 1963; Merrill, et al, 1965; Benis and LaCoste, 1968) have

provided convincing evidence indicating that blood has a yield stress, which is the minimum stress that must be overcome for flow to occur. The methods employed to demonstrate blood yield stress have been both direct application of torque-time measurements and indirect extrapolation of low shear rate data to zero flow.

The quantitative dependence of blood viscosity on shear rate and hematocrit will be readily apparent when actual viscometer data are presented in the experimental results. This qualitative discussion is given only to alert the reader to the complexities of blood rheology and the general factors which affect it.

At the outset it was also mentioned that analysis of blood flow in the human body is complicated considerably by the complexity of the circulatory system. That is, as the blood travels through the circulatory system it passes through vessels that vary considerably in size and geometry. For example, the blood may pass through a large, essentially straight vessel such as the aorta or a small, highly branched series of capillaries. Furthermore, the elastic nature of most blood vessels makes it impossible to generalize about size and geometry since both will vary locally with rate of flow.

One aspect of the circulation that has received much attention in recent years is the so-called microcirculation, a generic term referring to any and all of the small blood vessels including arterioles, capillaries, and venules. The quantitative study of the microcirculation is difficult since the diameter of these blood vessels is on the same order as the diameter of an erythrocyte. Hence, continuum fluid mechanics or theoretical equations of motion cannot be rigidly applied. This problem has been circumvented by either employing macroscopic empirical correlations or applying continuum mechanics anyway realizing the limitations of the approach. At any rate, the application of rheological data to blood flow in the microcirculation is limited and the work that has been done is conflicting and indicative of the complexity of the problem. Thus, a brief review of this work will point out the complex questions that have been raised and the incentive behind the research reported herein.

Workers in the laboratory of Bjorn Folkow at the University of Goteborg, Sweden, have reported (Djojosugito, et al, 1970) comparisons between blood viscosity <u>in vivo</u> ("apparent viscosity") and <u>in vitro</u> blood viscosity measured in a cone-plate viscometer. The <u>in vivo</u> viscometer was the

maximally dilated calf muscle vascular bed of the cat. The apparent *in vivo* viscosity was determined by comparing pressure flow relationships for blood and a Newtonian fluid assuming a linear pressure flow relationship for a constant vascular geometry. It was found that apparent *in vivo* viscosity was much lower than *in vitro* viscometer values at relatively high shear rates (230 sec^{-1}). This discrepancy was rationalized by assuming that the small vessels had favored local reductions in erythrocyte concentration as reported *in vitro* by Fahraeus and Lindqvist(1931).

On the other hand, workers at Columbia University's Laboratory of Hemorheology have reported (Benis, Usami, and Chien, 1972) a method of analysis that results in no apparent discrepancy between *in vivo* viscosity and *in vitro* viscometer data. Benis and co-workers studied steady blood flow in an isolated canine hindpaw and considered the situation to be similar to flow through a packed bed in which viscous and inertial pressure losses often occur simultaneously. Thus, the total pressure loss can be considered to be the sum of viscous and inertial pressure losses. That is,

$$\Delta P = \Delta P_v + \Delta P_i \qquad (1)$$

or

$$\Delta P = A\mu_a V + BV^2 \qquad (2)$$

where μ_a is the mean apparent viscosity of blood in the vascular bed and V is the volumetric flow rate. A and B are considered to be geometrical parameters that are a function of ΔP only. Utilization of Eq. (2) to determine apparent in vivo viscosity yielded results that agreed relatively well with in vitro viscometer data at comparable shear rates. Recall that the Swedish investigators had assumed a linear pressure flow relationship accounting only for the presence of viscous pressure losses whereas Benis and co-workers have included a term to account for possible inertial pressure losses.

The conflict existing between the Swedish investigators and the workers at Columbia has raised numerous questions that can only be resolved by a more systematic and objective approach. The model of Benis and co-workers suggests that much could possibly be learned by examining blood flow in a packed column wherein the flow is not complicated by changing vascular geometry. Thus, the research reported in these pages is hopefully a quantitative and objective consideration of blood flow in a packed bed of glass spheres.

Specifically, the research has been directed towards resolving two fundamentally important questions:

1) Can a workable model be developed to accurately correlate macroscopically the flow of blood in a packed bed?
2) Can the macroscopic model be extended to analysis of the microscopic behavior of blood within the bed?

It should be noted that the analysis of Newtonian flow in packed beds has been extensively studied and is of general importance in chemical engineering. However, non-Newtonian flow through packed beds is considerably more complicated and has received little attention.

THEORETICAL CONSIDERATIONS

Newtonian Flow Through Packed Beds

Newtonian flow through packed beds can be adequately correlated over the entire range of Reynolds numbers by an expression proposed by Ergun(1952),

$$\frac{\Delta P g_c D_p \epsilon^3}{L \rho U^2 (1-\epsilon)} = \frac{150}{(D_p U \rho)/\mu (1-\epsilon)} + 1.75 \qquad (3)$$

where

ΔP = pressure drop across bed, dynes/cm^2

g_c = constant, 1 (g-cm)/(dyne-sec^2)

D_p = effective particle diameter, cm

ϵ = void fraction, dimensionless

L = effective length of bed, cm

ρ = fluid density, g/cm^3

U = overall bulk average velocity, cm/sec

μ = fluid viscosity, poise=g/(cm-sec)

or in terms of modified friction factor and modified Reynolds number

$$f_m = 150/Re_m + 1.75 \qquad (4)$$

where

$$f_m = \frac{\Delta P g_c D_p \epsilon^3}{4\rho U^2 (1-\epsilon)} \tag{5}$$

and

$$Re_m = \frac{D_p U \rho}{\mu (1-\epsilon)} \tag{6}$$

Although Eq. (3) is essentially empirical in nature, it does have some theoretical basis by considering the packed column to be a composite of tortuous tubes of irregular cross-section; the overall equation is then obtained by applying results for single tubes to the composite. Nevertheless, empirical corrections must be considered to obtain an expression that accurately correlates experimental data. Such an analysis has been given by Bird, Stewart, and Lightfoot(1960).

It should be noted that the Ergun equation, Eq. (3), is simply the algebraic sum of two simplified expressions describing laminar and turbulent flow respectively. That is, laminar flow through a packed bed at $Re_m<1$ can be adequately described by the Kozeny-Carman equation

$$f_m = 150/Re_m \tag{7}$$

Eq. (7) states that the flow rate is proportional to the

pressure drop, which is Darcy's law. On the other hand, turbulent flow through a packed bed at $Re_m > 2000$ can be adequately correlated by the Burke-Plummer equation

$$f_m = 1.75 \tag{8}$$

The Ergun equation describing intermediate flow regimes ($1 < Re_m < 2000$) is then the sum of the Kozeny-Carman equation for laminar flow and the Burke-Plummer equation for turbulent flow. The general behavior of Newtonian flow through packed beds is depicted in Fig. 1, p. 13, by plotting f_m vs. Re_m on a log-log scale.

Non-Newtonian Flow and the Capillary Model

The correlation of non-Newtonian flow in packed beds is obviously quite complex since it will be characterized by local variations in shear rate and effective viscosity. The limited analysis of such flow reported in the literature thusfar has been confined to attempts to modify friction factor-Reynolds number expressions so that they adequately fit experimental observations. Sadowski and Bird(1965) have proposed a method for correlating the laminar flow of viscoelastic polymer solutions through packed beds by introducing another dimensionless group, the Ellis number, to describe the viscoelastic effects. Christopher and

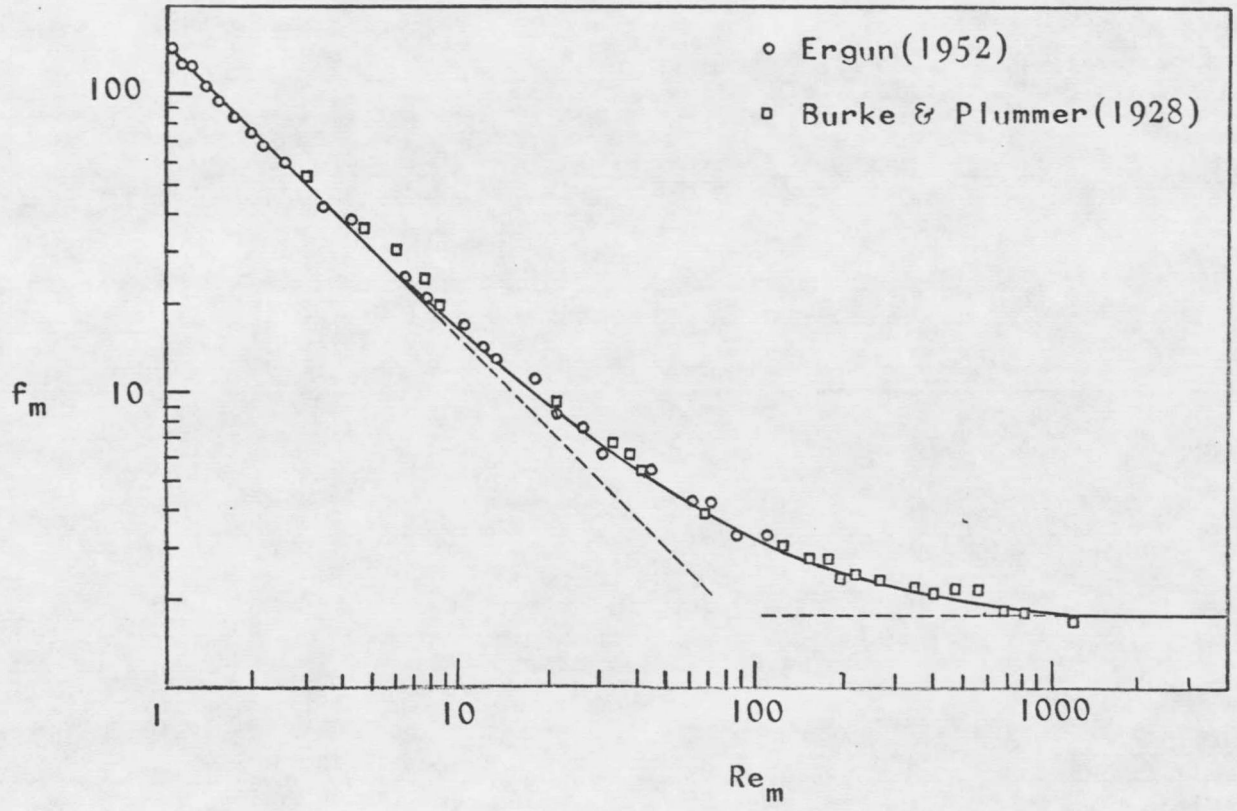

Figure 1. General behavior of Newtonian flow through packed beds. (Redrawn from Bird, Stewart, and Lightfoot, 1960).

Middleman(1965) have developed a modified Kozeny-Carman equation to describe the laminar flow of a power-law fluid through a packed bed. Gregory and Griskey(1967) have applied a similar approach to the flow of molten polymers.

Since blood does not apparently exhibit thixotropic or rheopectic effects, it can be considered rheologically a time-independent fluid. Thus, the primary problem in correlating blood flow in a packed bed is defining and quantifying shear stress, shear rate, and corresponding viscosity. These rheological parameters will, in general, vary locally throughout the bed even at a steady rate of bulk flow. Hence, any workable model of blood flow in a packed bed must necessarily resort to the use of average, yet physically realistic, values of these parameters.

Keeping the aforementioned limitations in mind, a workable model of blood flow in packed beds will now be developed. It is assumed that the packed bed can be viewed as a series of single tubes arranged in a tortuous, irregular manner. Equations describing non-Newtonian flow in a single pipe can then be used to estimate shear stress, shear rate, and corresponding effective viscosity as the blood flows through a single pore within the bed. The effective viscosity can then be used in a friction factor-Reynolds number

relationship. Such an approach can appropriately be termed a "capillary model" and is similar in principle to the approach of Bird, Stewart, and Lightfoot(1960) mentioned previously in conjunction with Newtonian flow.

The steady, laminar flow of a non-Newtonian fluid in a straight pipe can be described by the Rabinowitsch-Mooney relation (see Rabinowitsch, 1929; Mooney, 1931)

$$\gamma_w = \frac{3}{4}\frac{8U}{D} + \frac{1}{4}\tau_w \frac{d(8U/D)}{d\tau_w} \tag{9}$$

and

$$\tau_w = \frac{D(\Delta P)}{4L} \tag{10}$$

where

γ_w = shear rate at the wall, sec^{-1}

τ_w = shear stress at the wall, $dynes/cm^2$

U = overall bulk average velocity, cm/sec

D = diameter of pipe, cm

L = axial distance, cm

ΔP = axial pressure drop for two points a distance L apart, $dynes/cm^2$

The derivation of Equations (9) and (10) is given in the Appendix. Equations (9) and (10) are very powerful tools

for analysis of flow in pipes since they are independent of fluid properties. The only restriction in addition to steady, laminar flow is that the shear rate be a function only of shear stress. This restriction is probably not rigorously met for blood flow in extremely small tubes such as the vessels of the microcirculation since blood then cannot strictly be viewed as a homogeneous continuum.

Now, Equations (9) and (10) can be applied at a point in a packed bed as fluid moves through a single pore. That is,

$$\gamma_o = \frac{3}{4}\frac{8u}{D_o} + \frac{1}{4}\tau_o\frac{d(8u/D_o)}{d\tau_o} \qquad (11)$$

and

$$\tau_o = \frac{D_o}{4}\frac{dP}{dx} \qquad (12)$$

where

γ_o = shear rate at wall of pore, sec^{-1}

τ_o = shear stress at wall of pore, $dynes/cm^2$

u = local interstitial velocity, cm/sec

D_o = effective pore diameter, cm

$\frac{dP}{dx}$ = differential pressure gradient at pore, $dynes/cm^2/cm$

However, the local interstitial velocity, u, can be related to the overall bulk average velocity, U, by

$$u = U/\epsilon \tag{13}$$

Also

$$U = V/A_b \tag{14}$$

where V is the overall volumetric flow rate and A_b is the cross-sectional area of the bed. Thus,

$$u = \frac{V}{\epsilon A_b} \tag{15}$$

Furthermore, the differential pressure gradient at the pore can be considered constant along the axis of the bed so

$$\frac{dP}{dx} = \frac{\Delta P}{L} \tag{16}$$

where ΔP is the axial pressure drop across the effective length of the bed, L.

Now, substituting Equations (15) and (16) into Equations (11) and (12) gives

$$\gamma_o = \frac{3}{4}\frac{8V}{\epsilon A_b D_o} + \frac{1}{4}\tau_o \frac{d(8V/\epsilon A_b D_o)}{d\tau_o} \tag{17}$$

and

$$\tau_o = \frac{D_o}{4} \frac{\Delta P}{L} \tag{18}$$

Thus, the local shear rate and shear stress at the wall of a single pore within the bed have been related to the overall variables of flow. The only parameter in Equations (17) and (18) that does not lend itself to direct observation is the effective pore diameter, D_o. The resolution of this problem will be presented shortly.

Equations (17) and (18) can then be used to estimate the mean apparent viscosity for the fluid flowing through the bed. That is,

$$\mu_a = \frac{\tau_o g_c}{\gamma_o} \tag{19}$$

In reality, Eq. (19) gives the local viscosity at the wall of a single pore. However, it is felt that such a value should be reasonable to use in attempting to correlate pressure drop flow rate data. Thus, the mean apparent viscosity, μ_a, for blood flowing through a packed bed would, in general, vary with overall rate of flow but would be considered constant for a given rate of flow.

Using the concept of mean apparent viscosity it should be possible to correlate blood flow in a packed bed. That

is,

$$Re_m = \frac{D_p U \rho}{\mu_a (1-\epsilon)} \tag{20}$$

Hence, laminar blood flow should be described by a modified Kozeny-Carman equation

$$\frac{\Delta P g_c D_p \epsilon^3}{L \rho U^2 (1-\epsilon)} = \frac{150}{(D_p U \rho)/\mu_a (1-\epsilon)} \tag{21}$$

Turbulent blood flow should be described by the Burke-Plummer equation as for Newtonian flow since the fluid viscosity does not enter into the correlation. Blood flow in intermediate regions could then be described by a modification of the Ergun equation

$$\frac{\Delta P g_c D_p \epsilon^3}{L \rho U^2 (1-\epsilon)} = \frac{150}{(D_p U \rho)/\mu_a (1-\epsilon)} + 1.75 \tag{22}$$

Thus, the only modification that need be made for non-Newtonian blood flow is the determination of the appropriate mean apparent viscosity which is now a variable as are pressure drop and flow rate.

It should be noted the Eq. (22) can be rearranged to give

$$\Delta P = \frac{150L(1-\epsilon)^2}{g_c D_p^2}\mu_a U + \frac{1.75L\rho(1-\epsilon)}{g_c D_p \epsilon^3} U^2 \qquad (23)$$

Thus, it can readily be seen that the correlation proposed by Benis and co-workers to describe blood flow in the microcirculation, Eq. (2), is essentially the same as Eq. (23) which is proposed to adequately describe blood flow in a packed bed.

The effective pore diameter, D_o, can be determined by examining Newtonian flow through a packed bed. That is, for Newtonian flow

$$\frac{d(8V/\epsilon A_b D_o)}{d\tau_o} = \frac{8V/\epsilon A_b D_o}{\tau_o} \qquad (24)$$

so Eq. (17) becomes

$$\gamma_o = \frac{8V}{\epsilon A_b D_o} \qquad (25)$$

Thus, for Newtonian flow

$$\mu = \frac{\tau_o g_c}{\gamma_o} = \frac{D_o^2 \Delta P g_c \epsilon A_b}{32VL} \qquad (26)$$

so

$$D_o = \left(\frac{32\mu VL}{\Delta P g_c \epsilon A_b}\right)^{\frac{1}{2}} \qquad (27)$$

D_o should, of course, be constant for a given bed.

It is now useful to summarize the steps involved in the application of the capillary model to analysis of blood flow in a packed bed.

1) Obtain pressure drop flow rate data for a Newtonian fluid.
2) Determine D_o using Eq. (27).
3) Obtain pressure drop flow rate data for blood flow.
4) Determine shear rate and shear stress within the bed using Equations (17) and (18).
5) Determine mean apparent viscosity for each flow rate using Eq. (19).
6) Calculate modified friction factor and modified Reynolds number using Equations (5) and (20).
7) Plot friction factor vs. Reynolds number on a log-log scale to see if the appropriate relationship is satisfied.

EXPERIMENTAL APPARATUS AND PROCEDURE

Experimental Apparatus

A general schematic diagram of the experimental apparatus used is shown in Fig. 2, p. 23. Steady flow was initiated with a syringe pump (Harvard Apparatus Co., Model 902) utilizing 30 and 50 cm^3 gas-tight syringes (Hamilton Co., #1030 and #1050). The pressure drop across the column was monitored by a differential strain-gauge transducer (Statham Instruments, Inc., Model PL280TC) which converted the pressure drop to a corresponding electrical output that was then read on a universal transducer readout (Statham Instruments, Inc., Model SC1001). Standard luer-lok fittings were used in conjunction with polyethylene tubing (Becton, Dickinson and Co.) to connect the syringe to the column as well as to connect the pressure taps to the transducer.

A more detailed diagram of the column used is shown in Fig. 3, p. 24. The column was cast of clear lucite polymer with an inside bore diameter of 1.27 cm corresponding to a cross-sectional area of 1.267 cm^2. The pressure taps were 15.24 cm apart which, of course, was then the effective length of the column. Both ends of the column were threaded to fit a solid stainless steel end cap with luer-lok fitting (Millipore Corp., Model XX30 025 00). In addition, a teflon gasket, a porous stainless steel support plate, and a mesh

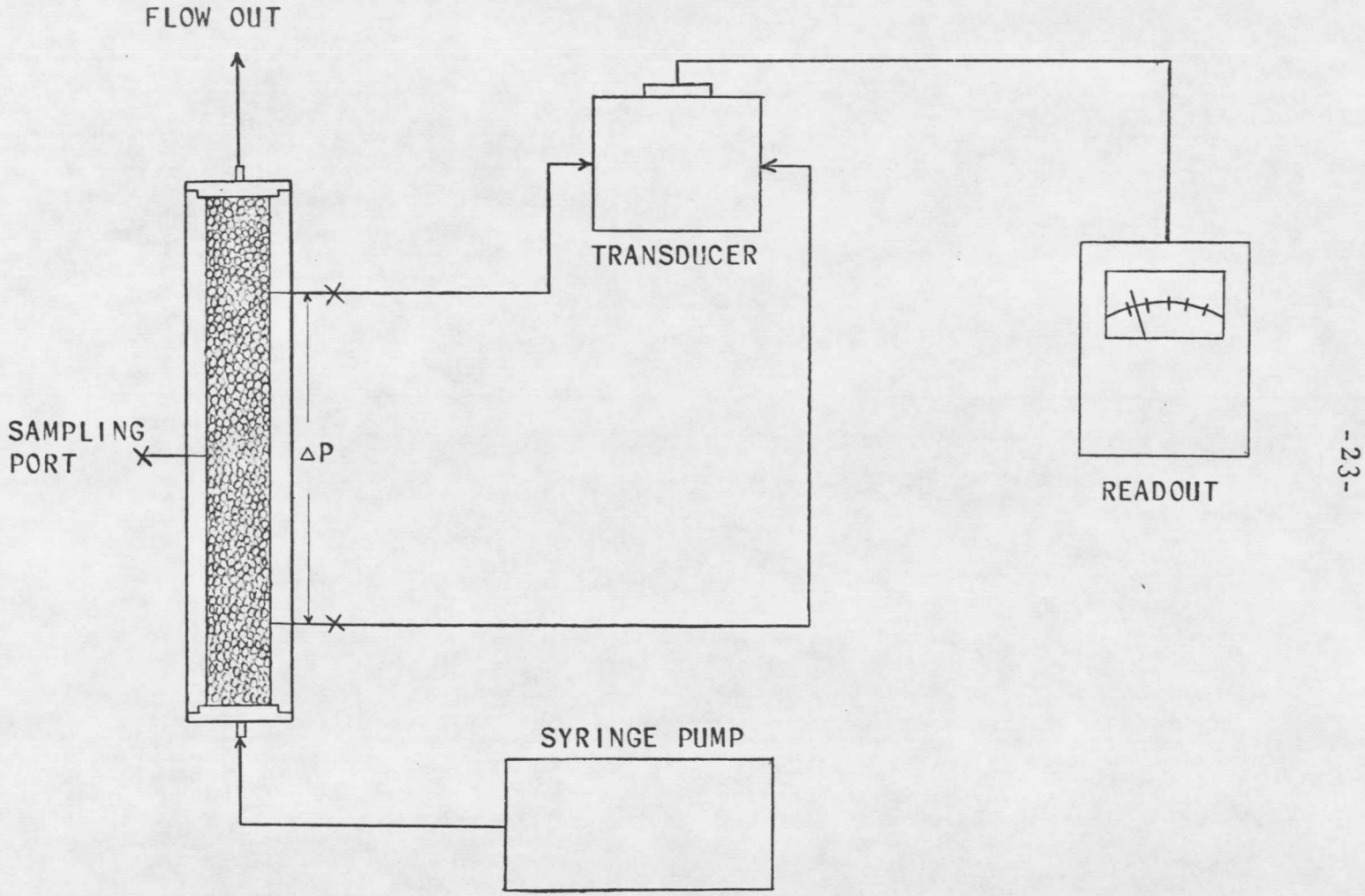

Figure 2. General schematic diagram of experimental apparatus.

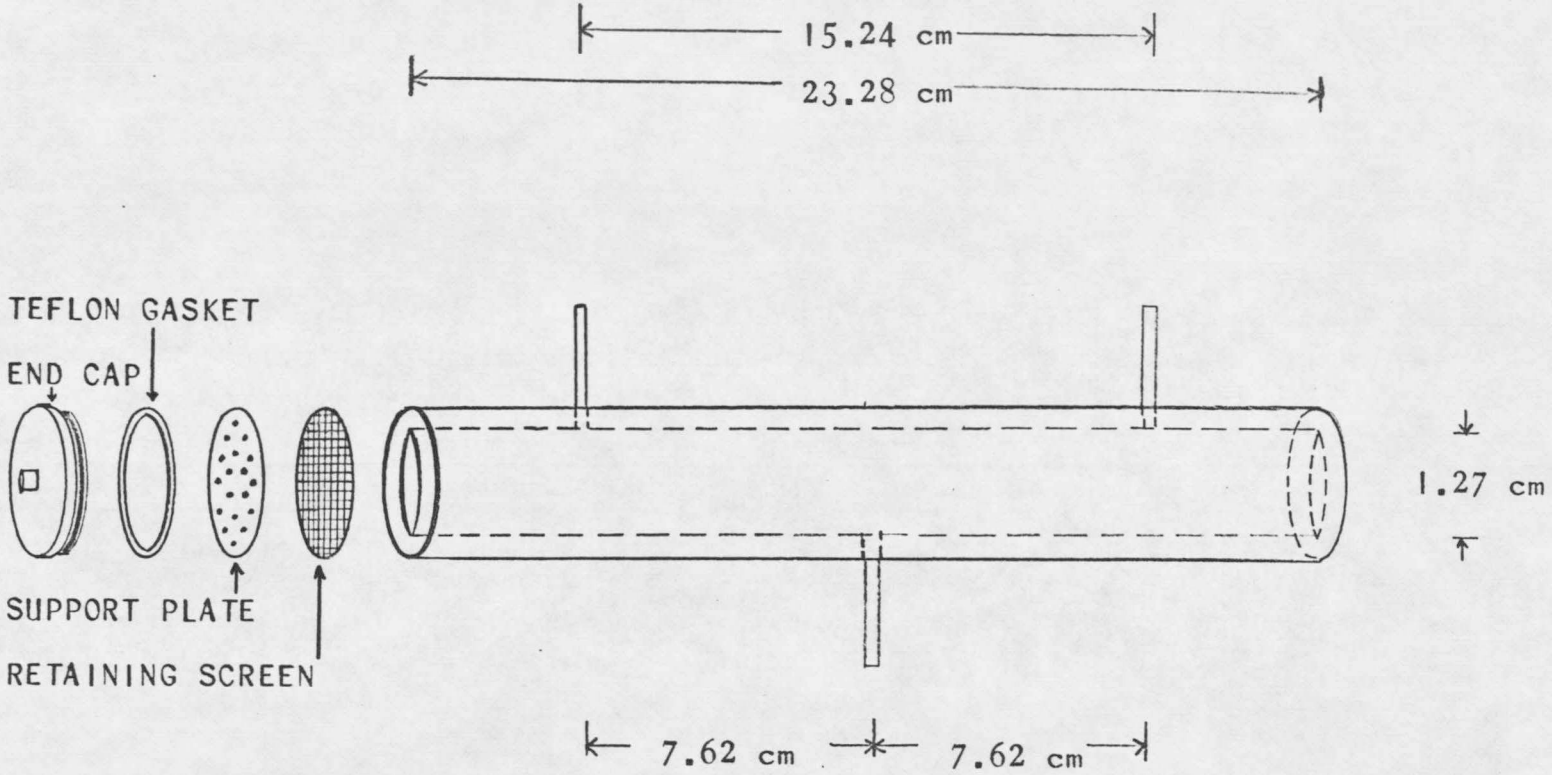

Figure 3. Schematic diagram of column used.

retaining screen were inserted as shown. The mesh retaining screen had openings of 44 microns which adequately retained the beads (diameter = 123 microns) but allowed complete passage of erythrocytes.

Blood

Blood was obtained in ACD anticoagulant from healthy humans by normal blood bank methods. Before utilizing blood in the packed column it was filtered through a Swank transfusion filter (Extracorporeal Medical Specialties, Inc., IL-200) to remove any protein or platelet aggregates that could possibly clog the column. In all cases the blood was utilized within 24 hours of its drawing.

Hematocrit was determined utilizing micro-hematocrit capillary tubes. The hematocrit of both the initial and exit blood was determined to ensure that no screening and retention of erythrocytes occurred. In all cases the initial and exit hematocrits were the same (±0.2%). Furthermore, the exit blood was examined microscopically to ensure that the erythrocytes were visibly intact and had not crenated.

Bead Analysis

The beads utilized in this investigation were rigid

SUPERBRITE glass spheres manufactured in controlled sizes by 3M Co., Reflective Products Division. The mean nominal diameter of the beads as stated by the manufacturer was 120 microns. A more exact size determination was accomplished by direct measurement of photomicrographs. That is, random samples of beads were placed under a microscope and photographed. Typical results are shown in Fig. 4, p. 27. Direct measurement of 100 beads from the photomicrographs yielded a mean diameter of 123.0 microns with a standard deviation of 8.7 microns. Examination of Fig. 4 qualitatively shows that the beads were indeed spherical and of a relatively uniform size.

Prior to use the beads were treated with a dilute solution of SILICLAD silicone concentrate (Clay Adams, Inc.), which prevented the possibility of any formed elements adhering to the glass surface of the beads.

Syringe Pump Calibration

The syringe pump was equipped with a multi-speed transmission and a gear train that enabled selection of 12 steady flow rates over a range of 5000 to 1. Although each setting corresponded to a nominal flow rate furnished by the manufacturer, the syringe pump was calibrated by timing the

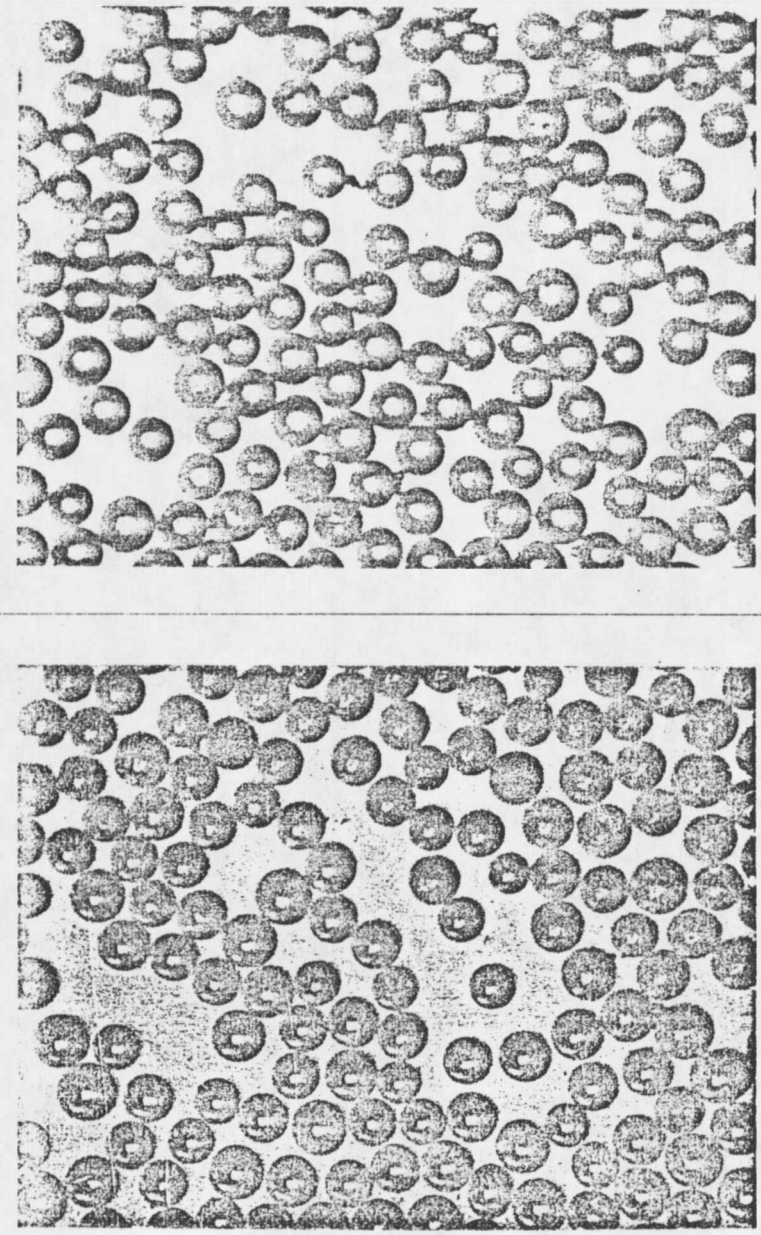

Figure 4. Photomicrographs of glass beads (70x).

outflow of water into a graduated cylinder. Twenty-one experimental calibration runs yielded a mean correction factor of 1.030 with a standard deviation of 0.010. The correction factor was defined as the experimentally determined flow rate divided by the nominal flow rate. Thus, each nominal flow rate was multiplied by the mean correction factor (1.030) to determine the actual flow rate.

Transducer Calibration

A general schematic diagram of the apparatus used to calibrate the transducer is shown in Fig. 5, p. 29. Compressed air was pushed through the column as shown thus initiating an equal pressure on the high pressure side of the transducer and on the high pressure side of a U-tube mercury manometer (Meriam Instrument Co., Model 20DA40). The low pressure side of each was open to atmospheric pressure. The transducer and readout were then calibrated from 0-60 inches of Hg and included 65 experimental readings. The calibration data obtained is plotted in Fig. 6, p. 30. A least squares straight line fitted to the data yielded the relation

$$\Delta P = .6194\ S + .001 \qquad (28)$$

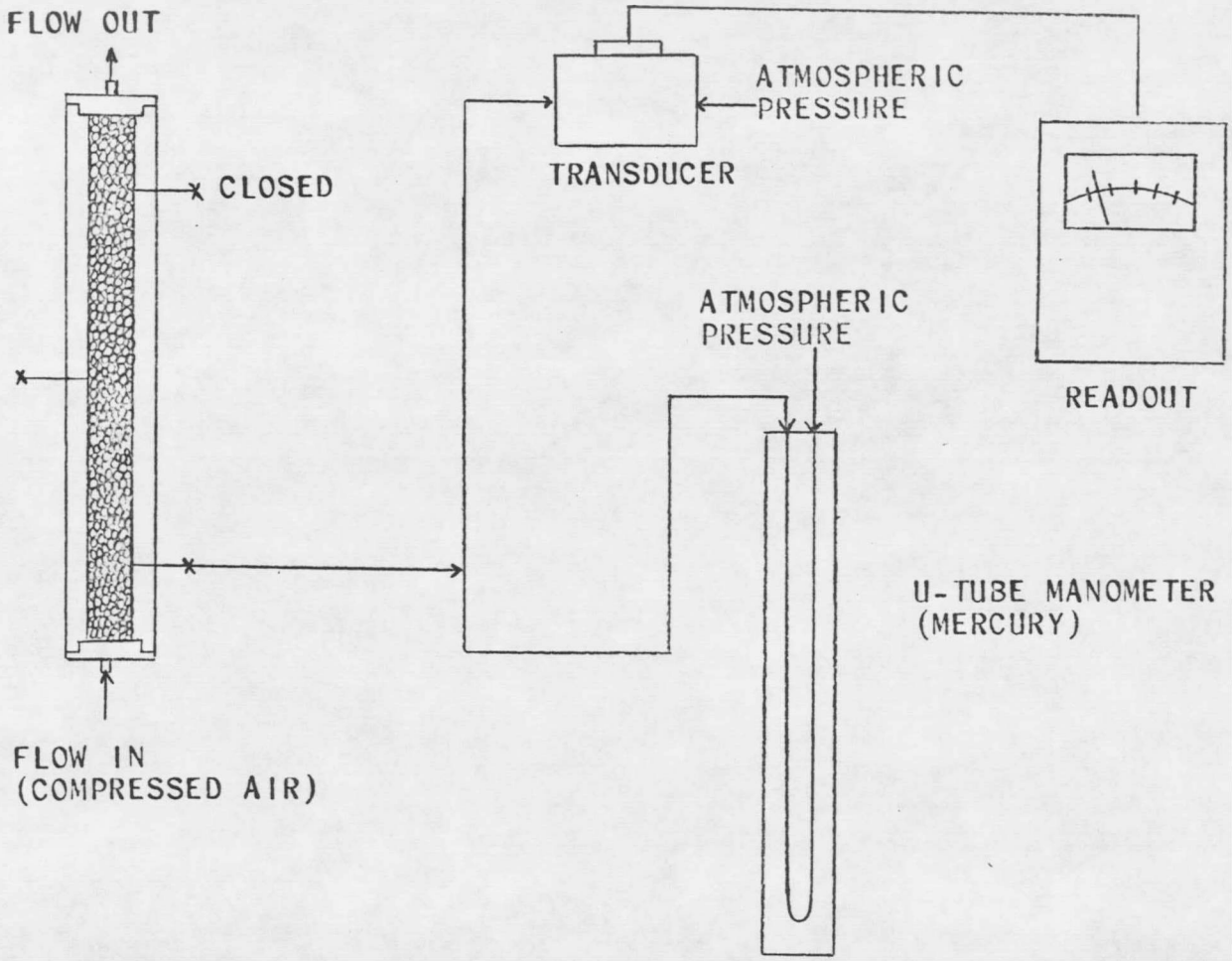

Figure 5. Schematic diagram of transducer calibration apparatus.

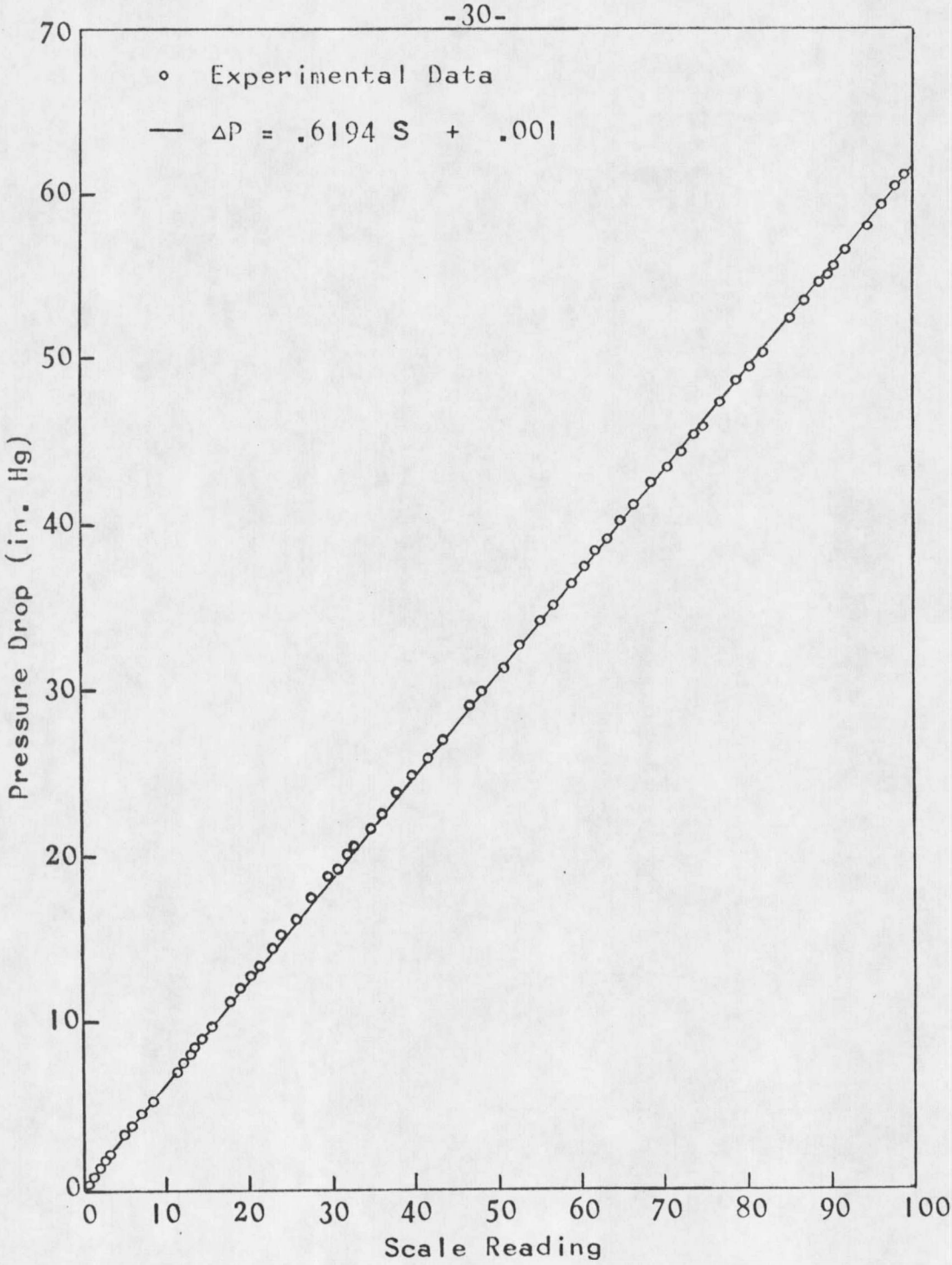

Figure 6. Transducer calibration data.

where ΔP is the pressure drop in inches of Hg and S is the scale reading. The line should ideally pass through the origin; however, the y-intercept, .001, represents a negligible contribution since the scale readings were from 1 to 100. The correlation coefficient for the calibration data was 0.998 indicating a very reliable linear relationship between pressure drop and scale reading over the entire range.

Entrance and Wall Effects

As shown in Fig. 2, the pressure taps were set in from the end of the column to ensure that the flow was fully developed and that no entrance effects produced experimental artifacts. However, a quantitative experiment was conducted as shown in Fig. 7, p. 32, to provide direct evidence that no entrance effects occurred. In one instance, as shown in Fig. 7(a), the pressure lines were connected to the lower pressure tap and to the sampling port; the pressure drop for six different flow rates of water was recorded. Similarly the experiment was repeated but with the pressure lines connected to the sampling port and to the upper pressure tap as shown in Fig. 7(b). It was found that the pressure drop across the lower portion of the column was identical to the

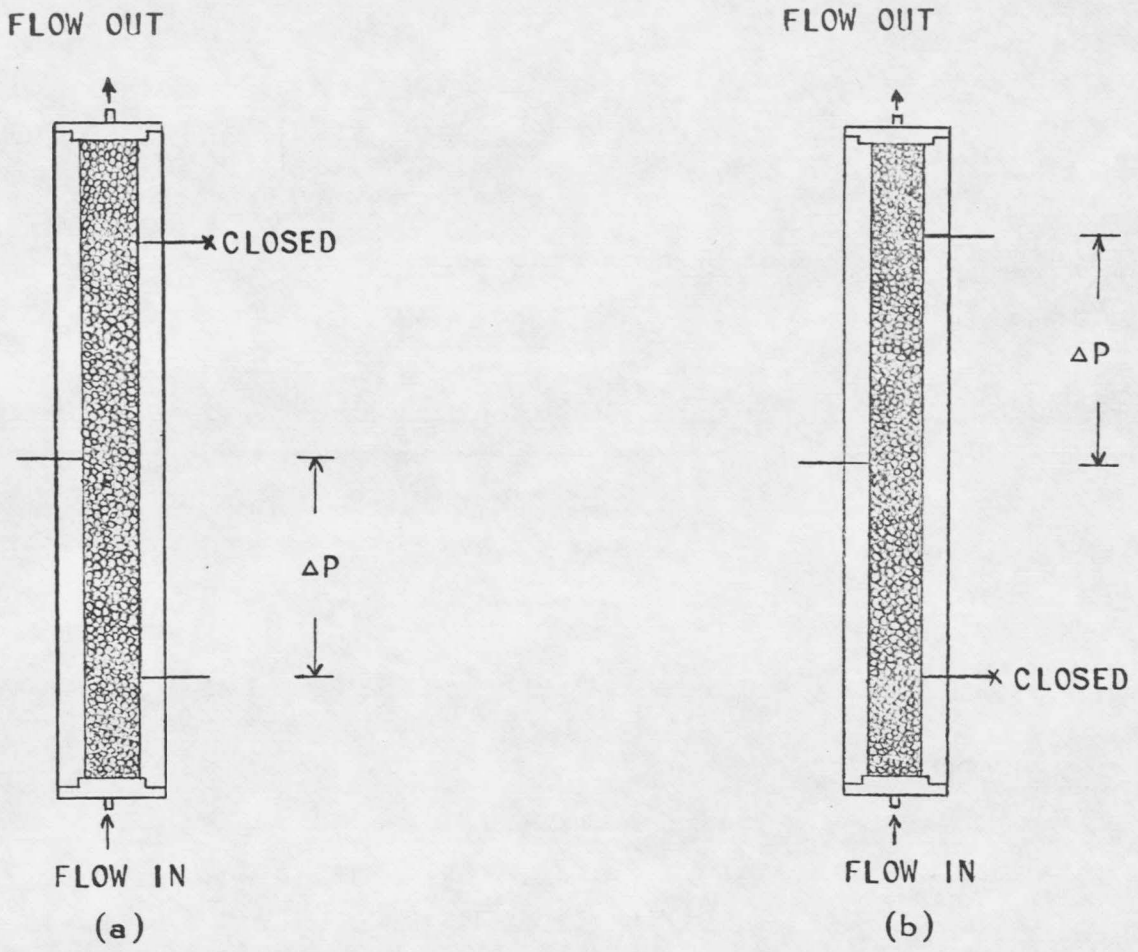

Figure 7. Experimental set-up utilized to examine possible entrance effects (see text for discussion).

pressure drop across the upper portion of the column at each of the six flow rates. In each case the effective length was the same (7.62 cm) since the sampling port was exactly midway between the pressure taps. Hence it was concluded that the flow was fully developed and that no entrance effects were present.

Mehta and Hawley(1969) have provided theoretical and experimental evidence indicating that if the ratio of column to particle diameter is greater than 50 to 1 then the wall effect is negligible and may be reasonably neglected. At column to particle diameter ratios less that this the frictional losses due to wall surface area constitute a signigicant portion of the total frictional losses and should not be neglected. However, in the present investigation the ratio of column to particle diameter was 103 to 1 so the frictional losses due to wall surface area were neglected.

Determination of Void Fraction

The void fraction, ϵ, is defined as

$$\epsilon = \frac{\text{volume void}}{\text{volume bed}} \tag{29}$$

or

$$\epsilon = \frac{\text{volume bed - volume particles}}{\text{volume bed}} \qquad (30)$$

But the particle volume is the mass of particles divided by the particle density. So,

$$\epsilon = \frac{\text{volume bed - particle mass/particle density}}{\text{volume bed}} \qquad (31)$$

Eq. (31) was utilized to determine the void fraction. The volume of the bed was 29.49 cm^3. The particle mass was determined by weighing the bed before and after filling. The particle density was 2.498 g/cm^3 as determined in a Le Chatelier specific gravity bottle by a previous investigator (Smith, 1972).

EXPERIMENTAL RESULTS AND DISCUSSION

Correlation of Newtonian Flow

As a preliminary to examination of non-Newtonian blood flow, data was obtained for the Newtonian flow of water through the packed column. In this way it was possible to verify the validity of the experimental apparatus and corresponding calibrations by comparing the data obtained to established Newtonian correlations. Also, the data for Newtonian flow is the basis for determining the effective pore diameter.

Table I, p. 36, presents the data obtained for the Newtonian flow of water through a bed with a void fraction of .3717. The modified friction factor was calculated utilizing Eq. (5). The overall bulk average velocity, U, was of course obtained by dividing the overall volumetric flow rate, V, by the cross-sectional area of the bed, A_b, as in Eq. (14). The modified Reynolds number was calculated utilizing Eq. (6). Fluid properties were obtained from Perry, Chilton, and Kirkpatrick(1963).

Since the modified Reynolds number is in all cases less than one the flow is laminar and should be described by the Kozeny-Carman equation, Eq. (7). Thus, the friction factor-Reynolds number product should be 150. Examination of

Table 1. Correlation of Newtonian water flow.
T=24.0°C ρ=.9973 g/cm^3
μ=.9142 cp ϵ=.3717

V(cm^3/min)	ΔP(mm Hg)	f_m	Re_m	$f_m \times Re_m$	% error
1.185	12.62	4578	.03330	152.4	1.60
1.525	15.77	3453	.04285	148.0	1.33
2.359	25.21	2307	.06628	152.9	1.93
3.801	39.37	1388	.1068	148.2	1.20
5.903	61.40	897.3	.1659	148.8	0.80
7.634	80.27	701.5	.2145	150.5	0.33
11.85	125.9	456.6	.3330	152.0	1.33
15.25	160.5	351.5	.4285	150.6	0.44
23.59	250.2	229.0	.6628	151.8	1.20
30.59	322.6	175.6	.8595	150.9	0.60

Table I shows excellent agreement with an average error of 1.07%. A plot of the experimental data as well as the Kozeny-Carman equation is given in Fig. 8, p. 38. The close correlation between the experimental data and the empirical equation would seem to verify the validity of the experimental apparatus.

Effective Pore Diameter

As was previously pointed out, it is possible to calculate an effective pore diameter that characterizes a given bed by examination of Newtonian flow. Recall,

$$D_o = \left(\frac{32\mu VL}{\Delta P g_c \epsilon A_b}\right)^{\frac{1}{2}} \qquad (27)$$

Eq. (27) was used to calculate an effective pore diameter for each of the data points presented in Table I. The results are tabulated in Table II, p. 39, along with the corresponding shear rate and shear stress at the wall of the pore.

The effective pore diameter should, of course, be constant for a given bed and be independent of the flow rate. The calculated values of D_o shown in Table II are essentially constant with the slight fluctuations well within the range of experimental error. The average of these values is 33.54 microns which will assumed to be the effective pore diameter

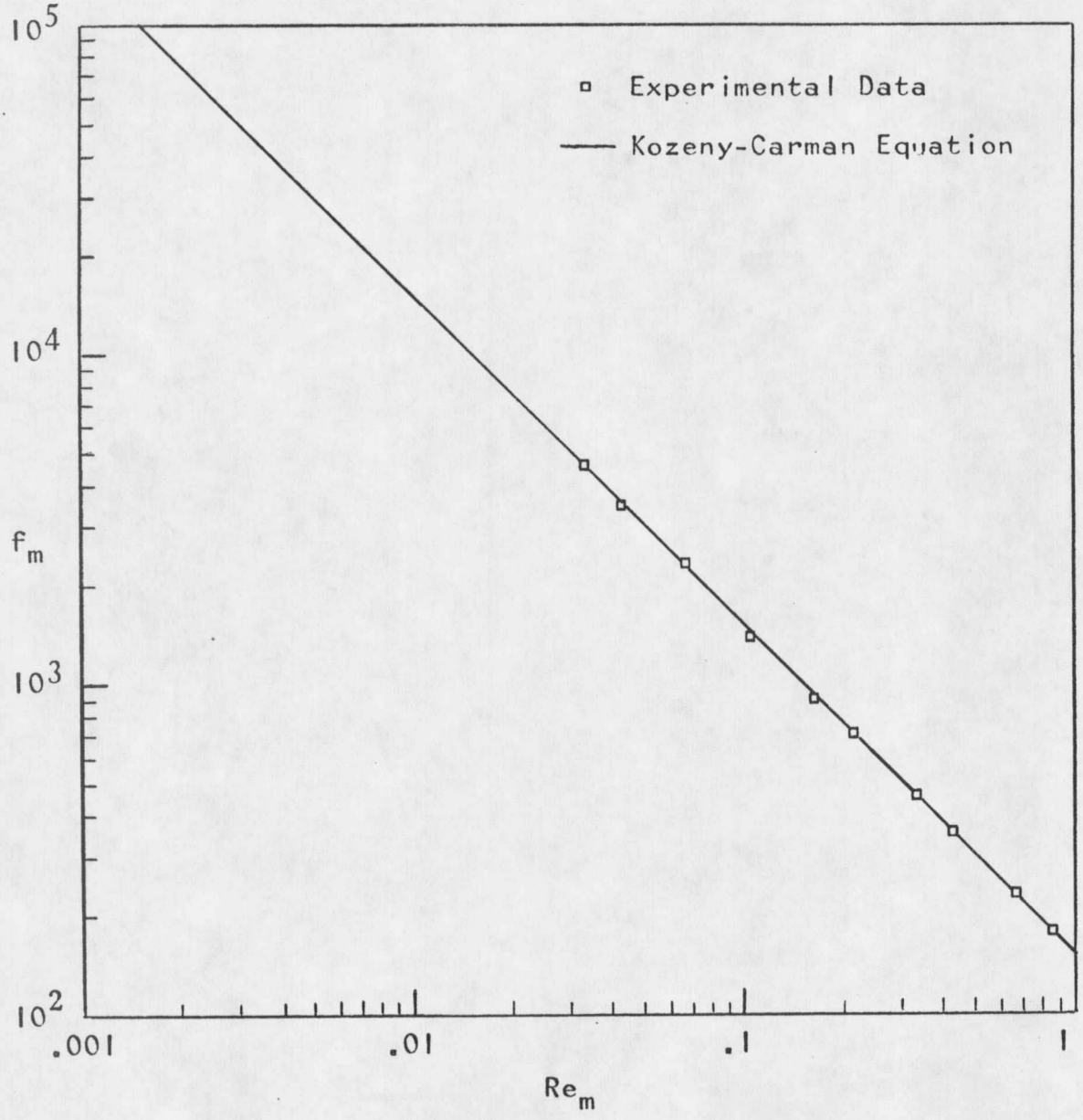

Figure 8. Modified friction factor vs. modified Reynolds number for laminar Newtonian flow of water.

Table II. Determination of effective pore diameter from Newtonian flow of water.
T=24.0°C ρ=.9973 g/cm^3
μ=.9142 cp ϵ=.3717

V(cm^3/min)	ΔP(mm Hg)	γ_o(sec^{-1})	τ_o(dynes/cm^2)	D_o(cm)
1.185	12.62	100.7	.9202	.003333
1.525	15.77	127.6	1.167	.003383
2.359	25.21	200.7	1.835	.003328
3.801	39.37	318.3	2.911	.003381
5.903	61.40	495.6	4.529	.003373
7.634	80.27	644.3	5.890	.003355
11.85	125.9	1005	9.191	.003338
15.25	160.5	1288	11.77	.003353
23.59	250.2	1999	18.28	.003341
30.59	322.6	2586	23.63	.003350

for a column with a void fraction of .3717.

Correlation of Blood Flow

Data obtained for blood flow through the packed column is presented in Tables III - X, pp. 41-48. Hematocrits of 16.8%, 34.5%, and 48.5% were considered. Blood (hematocrit= 40.3%) to which 0.5 weight % Dextran (molecular weight= 150,000; Pharmacia, Inc.) was added was also examined. Addition of Dextran to blood results in increased erythrocyte aggregation and plasma viscosity with a corresponding increase in overall viscosity.

The data has been correlated by application of the capillary model as previously outlined. In summary, the appropriate equations are

$$\gamma_o = \frac{3}{4}\frac{8V}{\epsilon A_b D_o} + \frac{1}{4}\tau_o \frac{d(8V/\epsilon A_b D_o)}{d\tau_o} \qquad (17)$$

$$\tau_o = \frac{D_o}{4}\frac{\Delta P}{L} \qquad (18)$$

$$\mu_a = \frac{\tau_o g_c}{\gamma_o} \qquad (19)$$

$$f_m = \frac{\Delta P g_c D_p \epsilon^3}{L\rho u^2 (1-\epsilon)} \qquad (5)$$

$$Re_m = \frac{D_p u \rho}{\mu_a (1-\epsilon)} \qquad (20)$$

(Text continued on page 49.)

Table III. Application of capillary model to blood flow, hematocrit=16.8%.
ϵ=.3713 D_o=33.5 microns T=23.7°C ρ=1.055 g/cm^3

V (cm^3/min)	ΔP (mm Hg)	$8V/\epsilon A_b D$ (sec^{-1})	τ_o (dynes/cm^2)	$\frac{d(8V/\epsilon A_b D_o)}{d\tau_o}$ (sec^{-1})	γ_o (sec^{-1})	μ_a (cp)
.7634	18.92	64.60	1.386	43.96	63.68	2.18
1.185	30.71	100.3	2.250	42.74	99.27	2.27
1.525	37.80	129.0	2.769	43.43	126.8	2.18
2.359	61.39	199.6	4.498	44.13	199.3	2.26
3.801	99.15	321.6	7.265	44.76	322.5	2.25
5.903	152.6	499.5	11.18	43.18	495.3	2.26
7.634	201.4	646.0	14.76	42.85	642.6	2.30
11.85	310.0	1002	22.71	43.92	1001	2.27
15.25	401.2	1290	29.40	43.72	1289	2.28
23.59	618.3	1996	45.30	42.90	1983	2.28
30.59	813.4	2588	59.60	42.90	2580	2.31

Table IV. Application of capillary model to blood flow, hematocrit=34.5%.
ϵ=.3760 D_o=33.9 microns T=25.0°C ρ=1.058 g/cm^3

V (cm^3/min)	ΔP (mm Hg)	$8V/\epsilon A_b D_o$ (sec^{-1})	τ_o (dynes/cm^2)	$\frac{d(8V/\epsilon A_b D_o)}{d\tau_o}$ (sec^{-1})	γ_o (sec^{-1})	μ_a (cp)
.3801	14.98	31.39	1.111	32.68	32.62	3.41
.5900	21.28	48.72	1.578	29.73	48.27	3.27
.7634	29.93	63.04	2.219	29.83	63.83	3.48
1.185	42.52	97.85	3.152	38.69	103.9	3.03
1.525	51.96	125.9	3.852	36.44	129.5	2.97
2.359	80.27	194.8	5.952	31.01	192.2	3.09
3.801	135.3	313.9	10.03	31.48	314.4	3.19
5.903	204.6	487.4	15.17	32.59	489.1	3.10
7.634	265.9	630.4	19.72	32.49	633.0	3.12
11.85	405.9	978.5	30.10	32.00	974.7	3.09
15.25	530.2	1259	39.31	31.92	1258	3.12
23.59	808.7	1948	59.96	32.37	1946	3.08
30.59	1057	2526	78.39	32.37	2529	3.10

Table V. Application of capillary model to blood flow, hematocrit=48.5%.
ϵ=.3744 D_o=33.8 microns T=24.3°C ρ=1.060 g/cm^3

V (cm^3/min)	ΔP (mm Hg)	$8V/\epsilon A_b D_o$ (sec^{-1})	τ_o (dynes/cm^2)	$\frac{d(8V/\epsilon A_b D_o)}{d\tau_o}$ (sec^{-1})	γ_o (sec^{-1})	μ_a (cp)
.3801	20.46	31.61	1.513	21.88	31.98	4.73
.5900	29.90	49.07	2.210	22.04	48.98	4.51
.7634	39.32	63.49	2.907	22.20	63.75	4.56
1.185	61.34	98.56	4.535	21.81	98.65	4.60
1.525	78.64	126.8	5.814	22.52	127.8	4.55
2.359	119.5	196.2	8.836	23.75	199.6	4.43
3.801	185.6	316.1	13.72	24.22	320.2	4.29
5.903	284.6	491.0	21.04	25.39	501.8	4.19
7.634	356.9	634.9	26.39	25.24	642.7	4.11
11.85	558.2	985.6	41.27	24.57	992.7	4.16
15.25	707.5	1268	52.31	24.97	1278	4.09
23.59	1093	1962	80.80	24.89	1974	4.09
30.59	1402	2544	103.7	24.89	2553	4.06

Table VI. Application of capillary model to blood flow, hematocrit=40.3% plus 0.5% Dextran.
ϵ=.3717 D_o=33.5 microns T=23.8°C ρ=1.059 g/cm^3

V (cm^3/min)	ΔP (mm Hg)	$8V/\epsilon A_b D_o$ (sec^{-1})	τ_o (dynes/cm^2)	$\frac{d(8V/\epsilon A_b D_o)}{d\tau_o}$ (sec^{-1})	γ_o (sec^{-1})	μ_a (cp)
.7634	42.52	64.45	3.119	21.44	65.06	4.79
1.525	81.85	131.9	6.004	22.38	132.5	4.53
3.801	199.8	320.9	14.66	23.31	326.1	4.50
7.634	380.8	644.5	27.93	23.76	649.3	4.30
15.25	759.9	1288	55.75	23.76	1297	4.30

Table VII. Correlation of blood flow, hematocrit=16.8%.
ϵ=.3713 D_o=33.5 microns
T=23.7°C ρ=1.055 g/cm^3

V (cm^3/min)	ΔP (mm Hg)	f_m	Re_m	$f_m \times Re_m$	% error
.7634	18.92	15565	.009509	148.0	1.33
1.185	30.71	10489	.01418	148.7	.87
1.525	37.80	7794	.01900	148.1	1.27
2.359	61.39	5291	.02834	150.0	.00
3.801	99.15	3291	.04587	151.0	.67
5.903	152.6	2101	.07093	149.0	.67
7.634	201.4	1657	.09013	149.4	.40
11.85	310.0	1059	.1418	150.1	.07
15.25	401.2	827.4	.1816	150.3	.20
23.59	618.3	532.9	.2810	149.7	.20
30.59	813.4	416.9	.3596	149.9	.07

Table VIII. Correlation of blood flow, hematocrit=34.5%.
ϵ=.3760 D_o=33.9 microns
T=25.0°C ρ=1.058 g/cm^3

V (cm^3/min)	ΔP (mm Hg)	f_m	Re_m	$f_m \times Re_m$	% error
.3801	14.98	51889	.003058	158.7	5.80
.5900	21.28	30583	.004951	151.4	.93
.7634	29.93	25697	.006019	154.7	3.13
1.185	42.52	15149	.01073	162.6	8.40
1.525	51.96	11178	.01409	157.5	5.00
2.359	80.27	7217	.02095	151.2	.80
3.801	135.3	4687	.03269	153.2	2.13
5.903	204.6	2937	.05225	153.5	2.33
7.634	265.9	2283	.06713	153.3	2.20
11.85	405.9	1446	.1052	152.2	1.47
15.25	530.2	1141	.1341	153.0	2.00
23.59	808.7	727.1	.2101	152.8	1.87
30.59	1057	565.3	.2707	153.1	2.07

Table IX. Correlation of blood flow, hematocrit=48.5%.
ϵ=.3744 D_o=33.8 microns
T=24.3°C ρ=1.060 g/cm^3

V (cm^3/min)	ΔP (mm Hg)	f_m	Re_m	$f_m \times Re_m$	% error
.3801	20.46	69660	.002203	153.5	2.33
.5900	29.90	42236	.003587	151.5	1.00
.7634	39.32	33180	.004590	152.3	1.53
1.185	61.34	21483	.007063	151.7	1.13
1.525	78.64	16629	.009190	152.8	1.87
2.359	119.5	10561	.01460	154.2	2.80
3.801	185.6	6316	.02429	153.4	2.27
5.903	284.6	4017	.03863	155.2	3.47
7.634	356.9	3012	.05093	153.4	2.27
11.85	558.2	1955	.07811	152.7	1.80
15.25	707.5	1496	.1022	153.0	2.00
23.59	1093	965.7	.1581	152.7	1.80
30.59	1402	737.1	.2066	152.3	1.53

Table X. Correlation of blood flow, hematocrit=40.3% plus 0.5% Dextran.
ϵ=.3713 D_o=33.5 microns
T=23.8°C ρ=1.059 g/cm^3

V (cm^3/min)	ΔP (mm Hg)	f_m	Re_m	$f_m \times Re_m$	% error
.7634	42.52	34956	.004351	152.1	1.40
1.525	81.85	16863	.009191	155.0	3.33
3.801	199.8	6628	.02306	152.8	1.87
7.634	380.8	3131	.04847	151.7	1.13
15.25	759.9	1566	.09682	151.6	1.07

The derivative appearing in Eq. (17) is the slope of a plot of $8V/\epsilon A_b D_o$ (ordinate) vs. τ_o (abscissa). However the derivative at a point n may also be approximated as

$$\left.\frac{d(8V/\epsilon A_b D_o)}{d\tau_o}\right|_n \doteq \frac{\dfrac{(8V/\epsilon A_b D_o)_n - (8V/\epsilon A_b D_o)_{n-1}}{(\tau_o)_n - (\tau_o)_{n-1}} + \dfrac{(8V/\epsilon A_b D_o)_{n+1} - (8V/\epsilon A_b D_o)_n}{(\tau_o)_{n+1} - (\tau_o)_n}}{2} \tag{32}$$

where n+1 represents a higher flow rate and n-1 a lower flow rate than point n. Eq. (32) was utilized to calculate values for the derivative appearing in Eq. (17).

Recall that an effective pore diameter of 33.54 microns was determined for a bed with a void fraction of .3717. However, analysis of each blood sample was characterized by a slightly different void fraction since the column was emptied and re-packed between runs. To account for this slight variation in void fraction an appropriate correction factor was applied. That is,

$$D_o = (33.54)\frac{\epsilon}{.3717} \tag{33}$$

where ϵ represents the void fraction of the bed for which

the effective pore diameter, D_o, is desired. Thus a bed with a void fraction greater than .3717 would have a correspondingly greater effective pore diameter. For example, the blood with hematocrit of 48.5% was analyzed in a bed with $\epsilon = .3744$, so the effective pore diameter used in correlating this data was $D_o = 33.54(.3744/.3717) = 33.8$ microns.

The density of the various blood samples was estimated from data given by Altman(1961).

Examination of Tables VII, VIII, IX, and X shows that the modified Reynolds number calculated with the mean apparent viscosity, μ_a, is less than one indicating laminar flow. Hence the friction factor-Reynolds number product should ideally be 150 as predicted from Eq. (21), the modified version of the Kozeny-Carman equation. The experimental results are seen to agree extremely well with this prediction with an average error of 1.87%. A graphical representation of the friction factor-Reynolds number relationship for each of the four blood samples examined is presented in Fig. 9, p. 51.

The accuracy with which the capillary model has been shown to correlate data would seem to indicate that it is a powerful tool in analyzing blood flow in a packed column. Indeed, this is certainly true on a macroscopic level.

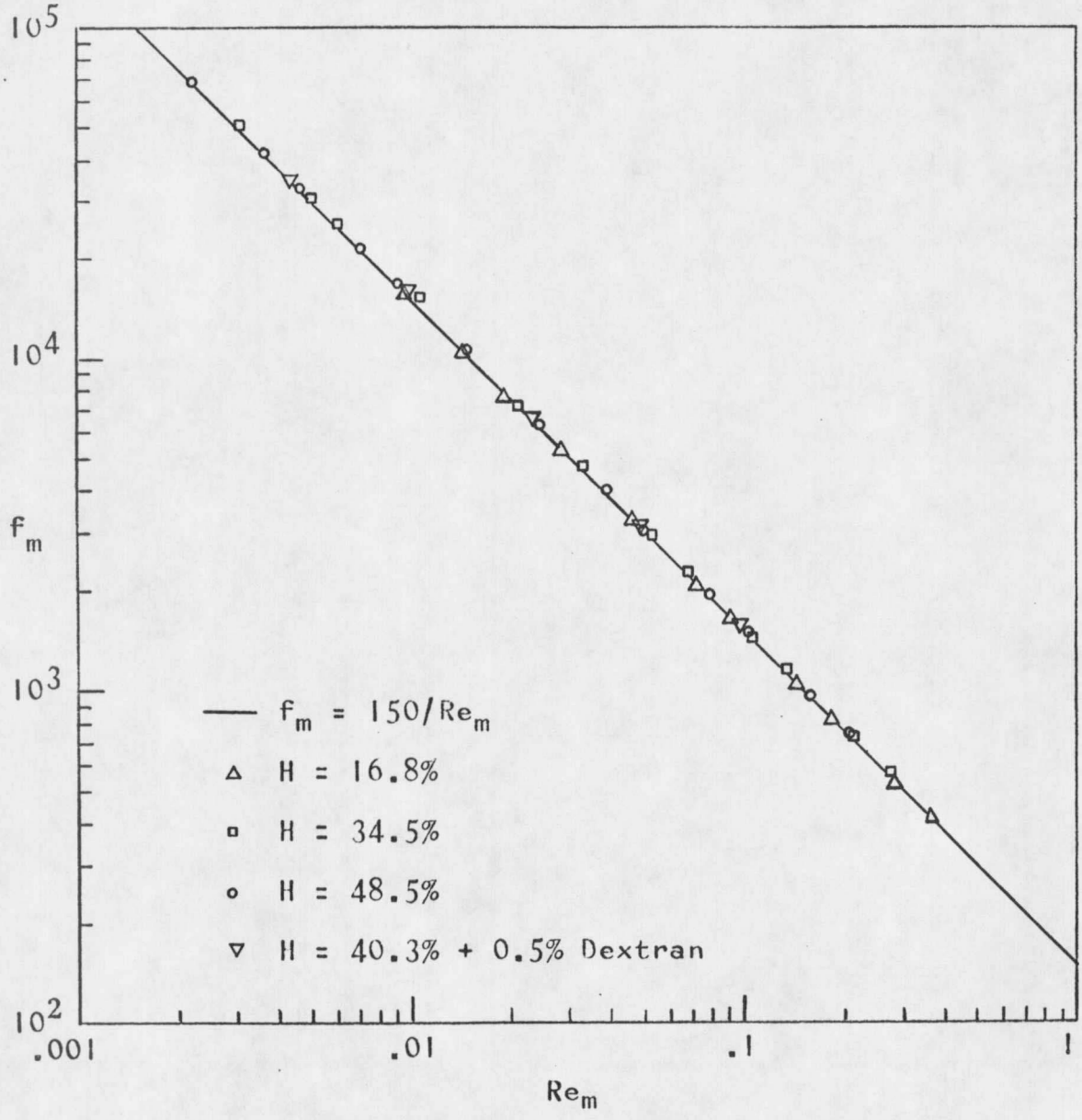

Figure 9. Modified friction factor vs. modified Reynolds number for laminar blood flow through a packed bed.

However, the method is only an approximation based on a model with inherent restrictions. Recall that each pore is analyzed as a single tube and that the bed is then viewed as a composite of single tubes. In itself, this is a reasonably accurate assumption. However, this means that one is now concerned with the analysis of blood flow in an extremely small tube (33-34 microns) which makes the assumption of a continuum fluid extremely tenuous if not totally inaccurate. Nevertheless, the capillary model involved application of the Rabinowitsch-Mooney relation which is based on continuum mechanics. Furthermore, the fact that the resulting model adequately correlates the macroscopic parameters of pressure drop and flow rate does not necessarily indicate assumptions made on a microscopic level are correct; it only indicates that the model is able to predict macroscopic behavior with reasonable accuracy.

In summary then, the capillary model should be considered only as an accurate method of correlating the macroscopic flow of blood in a packed column and not as a rigorous method of analyzing blood flow on a microscopic level. A particularly intriguing problem that arises on a microscopic level will now be considered.

The Packed Bed as a Viscometer

The astute observer may have noted that application of the capillary model to a packed bed means that each individual pore becomes, in essence, a crude tube viscometer. That is, the shear stress and shear rate at the wall of the pore are used to calculate a viscosity in a manner exactly analogous to that of a tube viscometer. Thus, viscosity as a function of shear rate as calculated with the capillary model (Tables III-VI) for each of the four blood samples analyzed is plotted in Fig. 10, p. 54.

Despite obvious fluctuations Fig. 10 reveals certain predictable trends. The viscosity is seen to increase markedly with hematocrit as would be expected. Furthermore, the non-Newtonian behavior of blood is exhibited since viscosity decreases as shear rate increases with an eventual leveling out to Newtonian behavior. A hematocrit of 16.8% is apparently sufficiently low to produce Newtonian behavior at the shear rates examined. One should note that addition of Dextran to blood with a hematocrit of 40.3% results in an effective viscosity higher than that for blood with a hematocrit of 48.5%. This is due to increased plasma viscosity as well as increased red cell aggregation.

One now might logically ask how the results presented

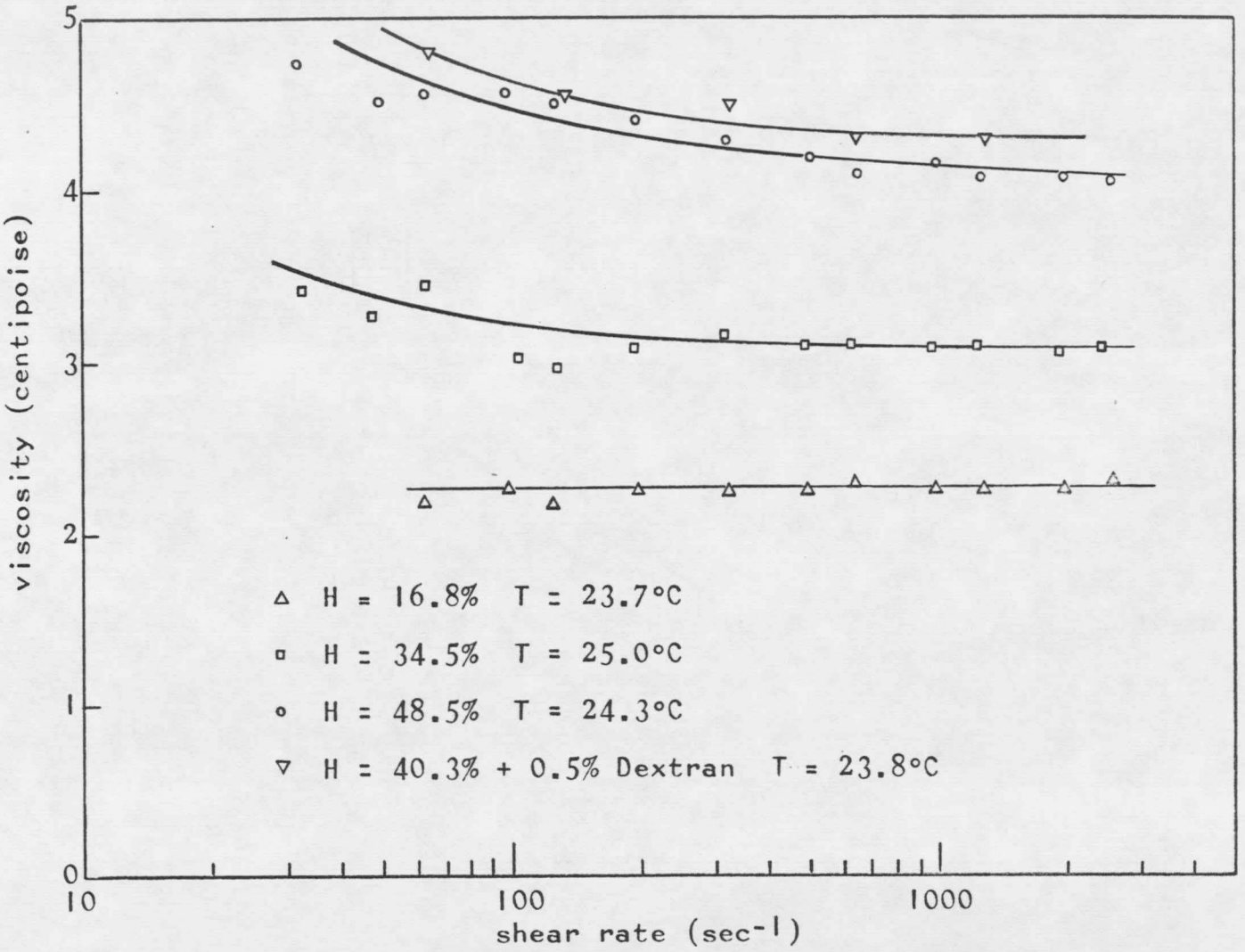

Figure 10. Blood viscosity vs. shear rate as calculated by capillary model.

in Fig. 10 agree with actual viscometer data. Such a comparison for each of the three normal blood samples analyzed is presented in Figs. 11, 12, and 13, pp. 56-58. Viscometer results have been interpolated from data recorded at 25.0°C at various hematocrits by Brooks, Goodwin, and Seaman(1970). Results for H=16.8% were interpolated between data for H= 8.25% and 18.2% while results for H=34.5% were interpolated between data for H=28.7% and 35.9%. Similarly, results for H=48.5% were interpolated between data for H=47.6% and 53.5%.

Examination of Figs. 11, 12, and 13 reveals an interesting yet perplexing trend. That is, a wide disparity exists between viscometer data and experimental calculations at lower shear rates; however, both viscometer data and experimental calculations seem to approach the same limiting Newtonian viscosity at hematocrits of 16.8% and 34.5%. The limiting viscosity for H=48.5% from viscometer data appears to be slightly higher than the limiting viscosity obtained from experimental calculations. One should note that comparisons at H=16.8% and H=48.5% are at slightly different temperatures; however the temperatures are sufficiently close to still render the comparisons meaningful.

The anomalies observed between viscometer data and experimental calculations using the capillary model are

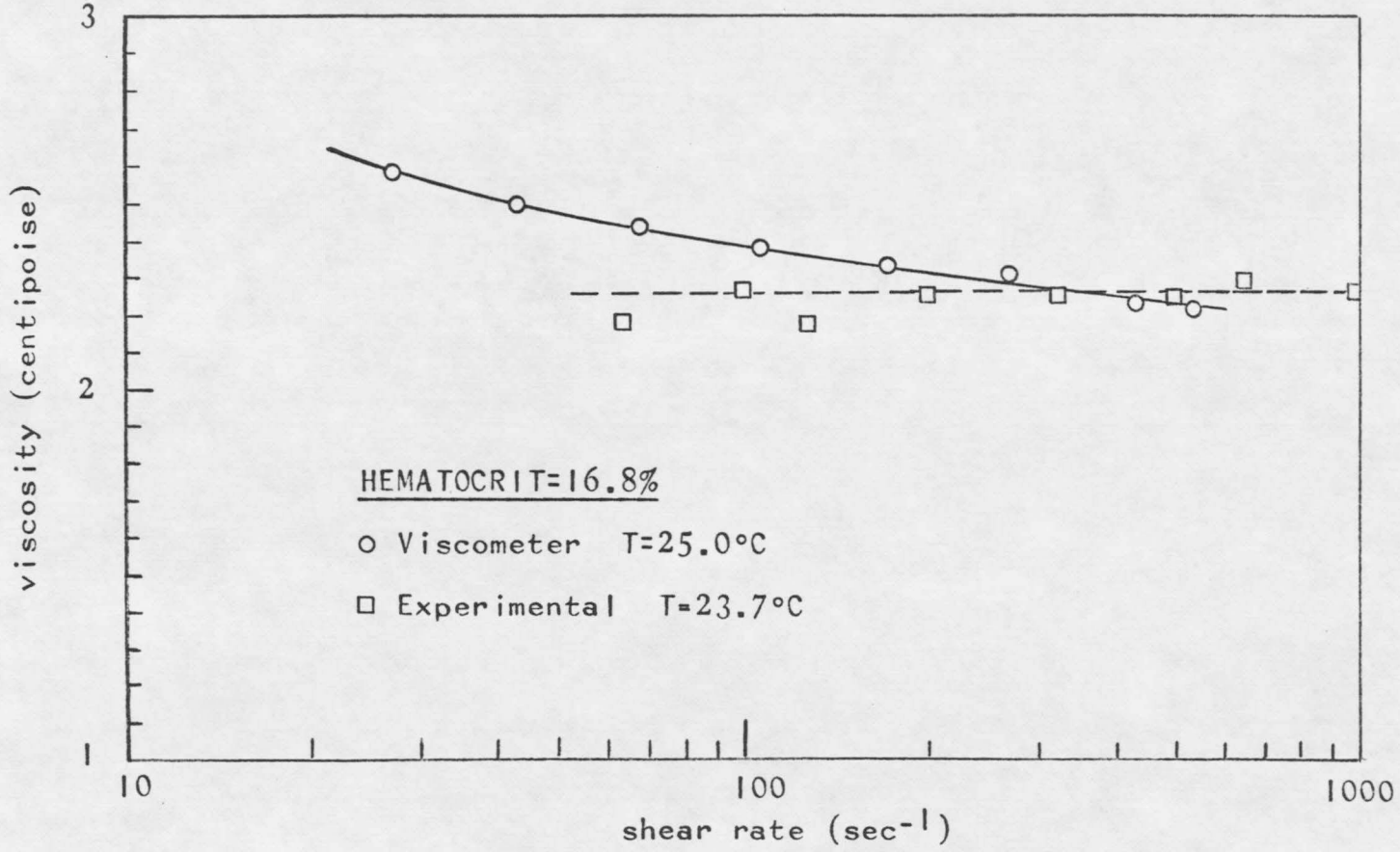

Figure 11. Comparison of experimental calculations to viscometer data, H=16.8%.

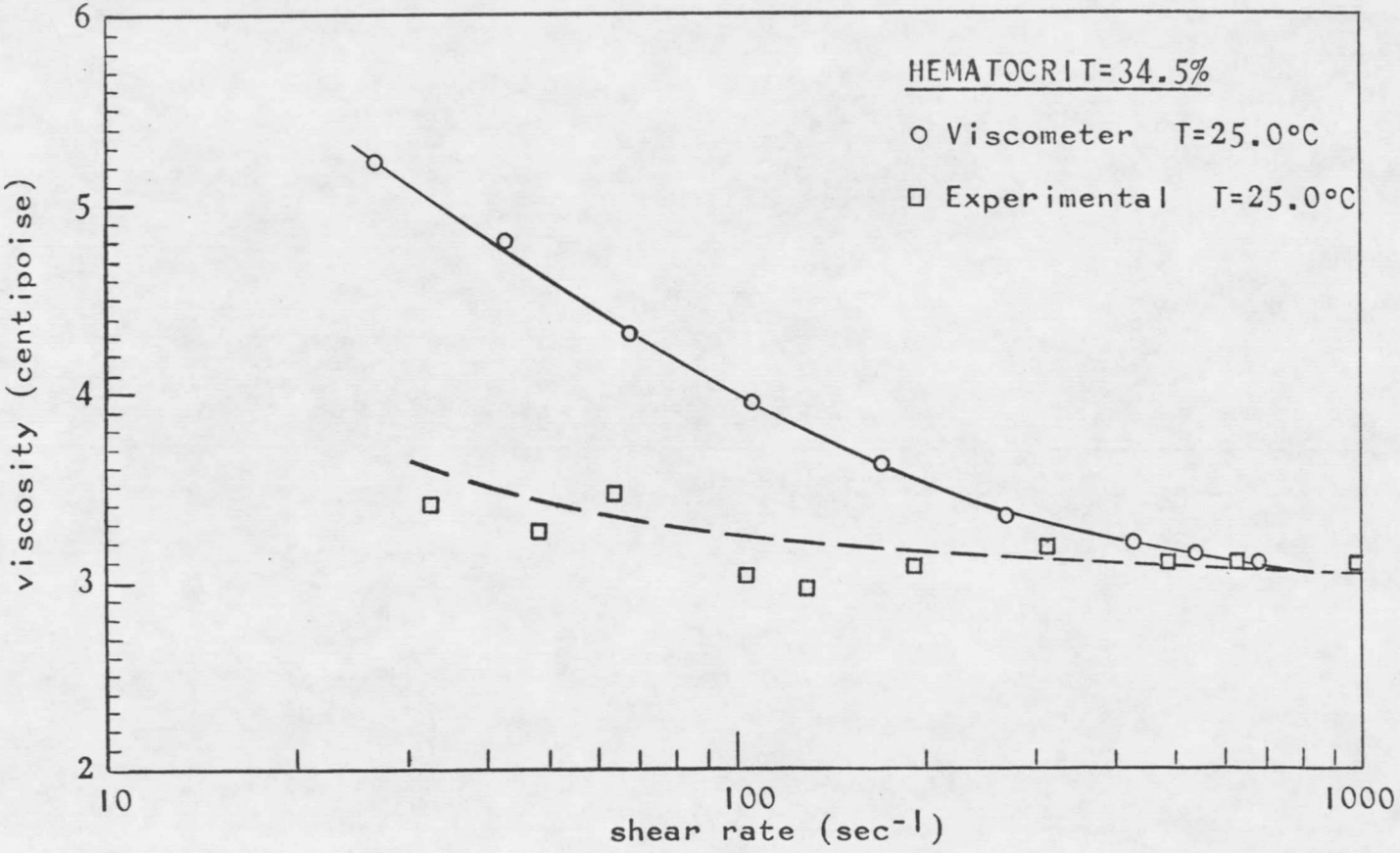

Figure 12. Comparison of experimental calculations to viscometer data, H=34.5%.

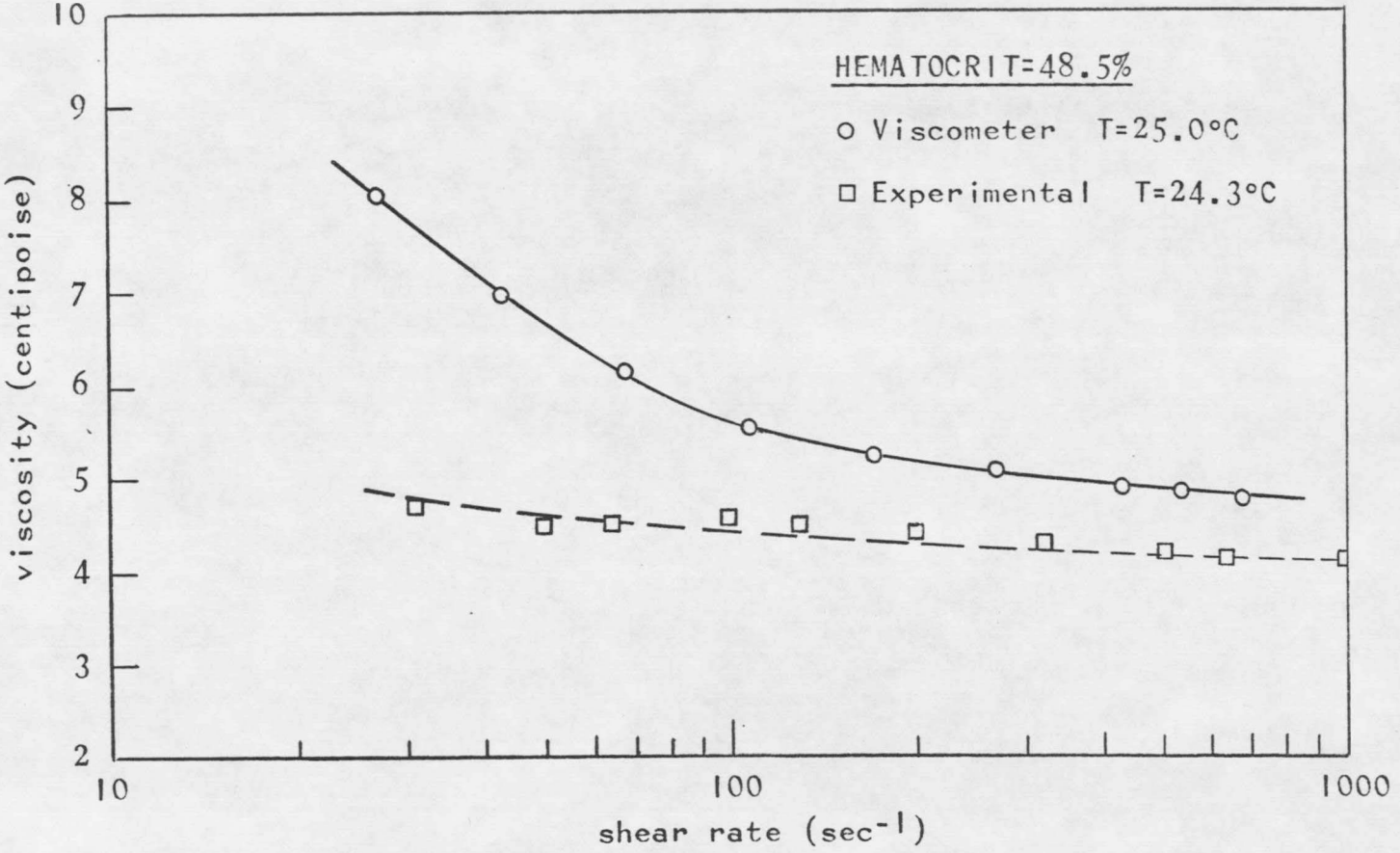

Figure 13. Comparison of experimental calculations to viscometer data, H=48.5%.

sufficiently nebulous to make an exact explanation impossible. However, in light of our present knowledge (or lack of it) concerning the microscopic behavior of blood, possible explanations rationalizing this anomalous behavior may be presented.

The small dimensions that characterize the pores of the column indicate that a local reduction in hematocrit could occur with a consequent decrease in viscosity (the Fahraeus effect). Such a reduction however would have to occur at the point of major resistance along the pore since a mass balance dictates that the overall hematocrit within the column remain the same. Furthermore, the Fahraeus effect would not explain why experimental calculations and viscometer data appear to approach essentially the same limiting Newtonian viscosity.

The non-Newtonian behavior of blood at decreasing shear rate is due to aggregation of red cells. Perhaps the tortuous, irregular nature of the bed coupled with the small pore size prevents the normal aggregation of red cells at decreasing shear rate. This possibility is rather doubtful but could be investigated by ascertaining data on the rate of red cell aggregation.

Certainly the most tenable and straight forward

explanation is that the capillary model fails to accurately predict behavior on a microscopic level due to the breakdown of continuum mechanics. Recall that the Rabinowitsch-Mooney relation required that the shear stress be a single valued function of shear rate at all points in the tube. Such an assumption verges on the ridiculous when considering blood flow in an extremely small pore such as 33-34 microns where the tube diameter is only about 4 times greater than the red cell diameter. Consequently, the assumption of a continuum fluid would understandably fail on this microscopic scale.

One fact clearly emerges from the results that have been presented thusfar: Although models based on continuum mechanics may satisfactorily correlate macroscopic properties, extension of the model to the microscopic level may not generally be valid. This failure is due primarily to a breakdown of continuum mechanics to describe microscopic behavior.

It should be noted in passing that the present investigation has not resolved the conflict existing between Swedish investigators and workers at Columbia concerning *in vivo* blood flow. However, it dramatically emphasizes the fact that extreme care should be taken in attempting to

describe microscopic blood flow with a macroscopic model, particularly in an *in vivo* situation where flow will be further complicated by changing vascular geometry.

Recommendations for Further Work

Only the steady, laminar flow of blood in a packed bed was considered in this investigation. It would be useful to investigate higher Reynolds numbers where inertial effects become important. Further investigations should also obtain direct viscometer data for the blood used in the column so a more meaningful comparison can be made between experimental calculations and viscometer data.

Further work should also be directed towards resolving the anomalies between viscometer data and experimental calculations. This requires accurate knowledge of what is happening on a microscopic scale as the blood flows through the pores of the bed. Such understanding will probably arise only after microscopic blood flow in simpler geometries such as the straight tube is further resolved.

Since the capillary model was developed for any time-independent non-Newtonian fluid and did not depend on any unique aspects of blood rheology, it would certainly seem that the analysis presented in this investigation could be applied to the flow of other non-Newtonian fluids through

packed columns and porous media. For example, the processing of many polymers often involves filtration through porous media or packed columns and thus constitutes a class of industrially important non-Newtonian flow that is not well understood. The capillary model may provide a method for predicting the macroscopic flow characteristics of such a system.

CONCLUSIONS

On the basis of the research that has been presented in these pages the two fundamental questions posed in the introduction can be answered.

1) The capillary model provides an accurate means of correlating pressure drop and flow rate for the steady, laminar flow of blood in a packed bed. As such, the method is very powerful since it is independent of hematocrit and does not require the use of viscometer data. Furthermore, the method should be applicable to the steady, laminar flow of other time-independent non-Newtonian fluids through a packed bed.

2) The capillary model cannot be readily extended to the prediction and understanding of what is occurring on a microscopic level as the blood flows through the individual pores of the bed. This is probably due to the failure of continuum mechanics to adequately describe blood flow in vessels whose characteristic diameter is on the same order of magnitude as an erythrocyte.

APPENDIX

Derivation of Rabinowitsch-Mooney Relation

Simple force and momentum balances for laminar, steady uniform flow in a circular pipe reduce to (see Longwell, 1966)

$$\frac{1}{r}\frac{d}{dr}(r\tau) = -\frac{dP}{dx} \qquad \text{(A-1)}$$

where r is the radial distance measured from the centerline, τ is the shear stress in the axial direction, and dP/dx is the axial pressure gradient. Integrating Eq. (A-1) with respect to r gives

$$\int_o^{r\tau} d(r\tau) = -\frac{dP}{dx}\int_o^r r\, dr \qquad \text{(A-2)}$$

or

$$r\tau = -\frac{dP}{dx}\frac{r^2}{2} \qquad \text{(A-3)}$$

Simplifying gives

$$\tau = \tau_w \frac{r}{r_o} \qquad \text{(A-4)}$$

where τ_w is the shear stress at the wall and r_o is the pipe radius. Similarly, the wall shear stress can be expressed as

$$\tau_w = \frac{D(\Delta P)}{4L} \tag{A-5}$$

which is Eq. (10) given in the main text.

Now assume that the shear rate is a function only of shear stress. That is,

$$-\frac{du_x}{dr} = \gamma = \Phi_2(\tau) \tag{A-6}$$

where u_x is the axial point velocity and $\Phi_2(\tau)$ denotes the yet unknown function of shear stress. From Eq. (A-4)

$$dr = \frac{r_o}{\tau_w} d\tau \tag{A-7}$$

Now, the volumetric flow rate through the pipe can be expressed as

$$V = \int_o^{r_o} u_x \, dA \tag{A-8}$$

But the differential area, dA, is simply

$$dA = 2\pi r \, dr \tag{A-9}$$

so

$$V = \int_o^{r_o} u_x \, 2\pi r \, dr = 2\pi \int_o^{r_o} u_x \, r dr \tag{A-10}$$

Integration of Eq. (A-10) by parts gives

$$V = 2\pi\left[\left\{u_x \frac{r^2}{2}\right\}_o^{r_o} - \int_o^{r_o} \frac{r^2}{2} \frac{du_x}{dr} dr\right] \tag{A-11}$$

However, if there is no slip at the wall $u_x=0$ when $r=r_o$ so

$$u_x \frac{r^2}{2}\Big|_o^{r_o} = 0 \tag{A-12}$$

Thus, Eq. (A-11) becomes

$$V = 2\pi\int_o^{r_o} \frac{r^2}{2}(-du/dr)dr \tag{A-13}$$

Substituting from Equations (A-4), (A-6), and (A-7) gives

$$V = 2\pi\int_o^{\tau_w} (r_o/\tau_o)^3 \tau^2/2 \, \Phi_2(\tau) \, d\tau$$

$$= \frac{\pi r_o^3}{\tau_o^3}\int_o^{\tau_w} \tau^2 \, \Phi_2(\tau) \, d\tau \tag{A-14}$$

Now let

$$V = 2\pi r_o^3 \, F(\tau_w) \tag{A-15}$$

where $F(\tau_w)$ denotes an unknown function of wall shear stress. Then

$$F(\tau_w) = \frac{V}{2\pi r_o^3} \tag{A-16}$$

So from Eq. (A-14)

$$F(\tau_w) = \frac{1}{\tau_w^3}\int_o^{\tau_w} \frac{\tau^2}{2}\,\Phi_2(\tau)\,d\tau \qquad (A\text{-}17)$$

Now, differentiate Eq. (A-17) with respect to τ_w to give

$$\frac{dF}{d\tau_w} = F' = -\frac{3}{\tau_w^4}\int_o^{\tau_w} \frac{\tau^2}{2}\,\Phi_2(\tau)d\tau + \frac{1}{\tau_w^3}\frac{d}{d\tau_w}\left[\int_o^{\tau_w} \frac{\tau^2}{2}\,\Phi_2(\tau)d\tau\right]$$

$$= -\frac{3F}{\tau_w} + \frac{1}{\tau_w^3}\left[\frac{\tau_w^2}{2}\,\Phi_2(\tau_w)\right] \qquad (A\text{-}18)$$

Thus

$$\Phi_2(\tau_w) = 6F + 2\tau_w F' \qquad (A\text{-}19)$$

The volumetric flow rate can be related to the overall bulk average velocity by

$$U = \frac{V}{\pi r_o^2} \qquad (A\text{-}20)$$

Substituting from Eq. (A-15) gives

$$U = 2r_o F = DF \qquad (A\text{-}21)$$

So

$$F = U/D \qquad (A\text{-}22)$$

Combining Equations (A-19) and (A-22) gives

$$\gamma_w = \Phi_2(\tau_w) = 6U/D + 2\tau_w \frac{d(U/D)}{d\tau_w} \qquad \text{(A-23)}$$

or equivalently

$$\gamma_w = \frac{3}{4}\frac{8U}{D} + \frac{1}{4}\tau_w \frac{d(8U/D)}{d\tau_w} \qquad \text{(A-24)}$$

which is Eq. (9) given in the main text.

LITERATURE CITED

Altman, P.L., Blood and Other Body Fluids, p. 12, Fed. Am. Soc. Exp. Biol. (1961).

Benis, A.M. and J. LaCoste, "Study of Erythrocyte Aggregation by Blood Viscometry at Low Shear Rates Using a Balance Method," Circ. Res., 22,29 (1968).

Benis, A.M., S. Usami and S. Chien, "Evaluation of Viscous and Inertial Pressure Losses in Isolated Tissue with a Simple Mathematical Model," Microvascular Res., 4,81 (1972).

Bird, R.B., W.E. Stewart and E.N. Lightfoot, Transport Phenomena, pp. 196-200, John Wiley & Sons, Inc., New York (1960).

Brooks, D.E., J.W. Goodwin and G.V.F. Seaman, "Interactions Among Erythrocytes Under Shear," J. Appl. Physiol., 28, 172 (1970).

Burke, S.P. and W.B. Plummer, "Gas Flow Through Packed Columns," Ind. Eng. Chem., 20,1196 (1928).

Charm, S. and G. Kurland, "Viscometry of Human Blood for Shear Rates of 0-100,000 sec^{-1}," Nature, 206,617 (1965).

Christopher, R.H. and S. Middleman, "Power-Law Flow Through a Packed Tube," Ind. Eng. Chem. Fund., 4:4,422 (1965).

Cokelet, G.R., "The Rheology of Human Blood," Sc.D. thesis, Mass. Inst. of Tech. (1963).

Cokelet, G.R., "The Rheology of Human Blood," In Y.C. Fung, N. Perrone and M. Anliker (ed.), Biomechanics: Its Foundations and Objectives, Prentice-Hall, Inc., Englewood Cliffs, N.J. (1972).

Djojosugito, A.M., B. Folkow, B. Oberg and S.W. White, "A Comparison of Blood Viscosity Measured In Vitro and in a Vascular Bed," Acta Physiol. Scand.,78,70 (1970).

Ergun, S., "Fluid Flow Through Packed Columns," Chem. Eng. Prog., 48,89 (1952).

Fahraeus, R. and T. Lindqvist, "The Viscosity of the Blood in Narrow Capillary Tubes," Amer. J. Physiol., 96,562 (1931).

Gregory, D.R. and R.G. Griskey, "Flow of Molten Polymers Through Porous Media," AIChE J., 13,122 (1967).

Longwell, P.A., Mechanics Of Fluid Flow, p. 40, McGraw-Hill, Inc., New York (1966).

Mehta, D. and M.C. Hawley, "Wall Effect in Packed Columns," Ind. Eng. Chem. Proc. Des. Dev., 8:2,280 (1969).

Merril, E.W., A.M. Benis, E.R. Gilliland, T.K. Sherwood and E.W. Salzman, "Pressure-Flow Relations of Human Blood in Hollow Fibers at Low Flow Rates," J. Appl. Physiol., 20,954 (1965).

Merril, E.W. and G.A. Pelletier, "Viscosity of Human Blood: Transistion from Newtonian to Non-Newtonian," J. Appl. Physiol., 23,178 (1967).

Merril, E.W., "Rheology of Blood," Physiol. Rev., 49,863 (1969).

Mooney, M., "Explicit Formulas for Slip and Fluidity," J. Rheol., 2,210 (1931).

Perry, R.H., C.H. Chilton and S.D. Kirkpatrick (ed.), Perry's Chemical Engineers' Handbook, 4 ed., McGraw-Hill, Inc., New York (1963).

Rabinowitsch, B., "Uber die Viskositat und Elastizitat von Solen," Z. Physik. Chem., A145,1 (1929).

Sadowski, T.J. and R.B. Bird, "Non-Newtonian Flow Through Porous Media," Trans. Soc. Rheol., 9:2,243 (1965).

Smith, J.H., "Rheology of Concentrated Suspensions of Spheres," Ph.D. thesis, Calif. Inst. of Tech. (1972).

Wayland, H., "Rheology and the Microcirculation," Gastroenterology, 52,342 (1967).

Whitmore, R.L., Rheology of the Circulation, Pergamon Press, Oxford (1968).